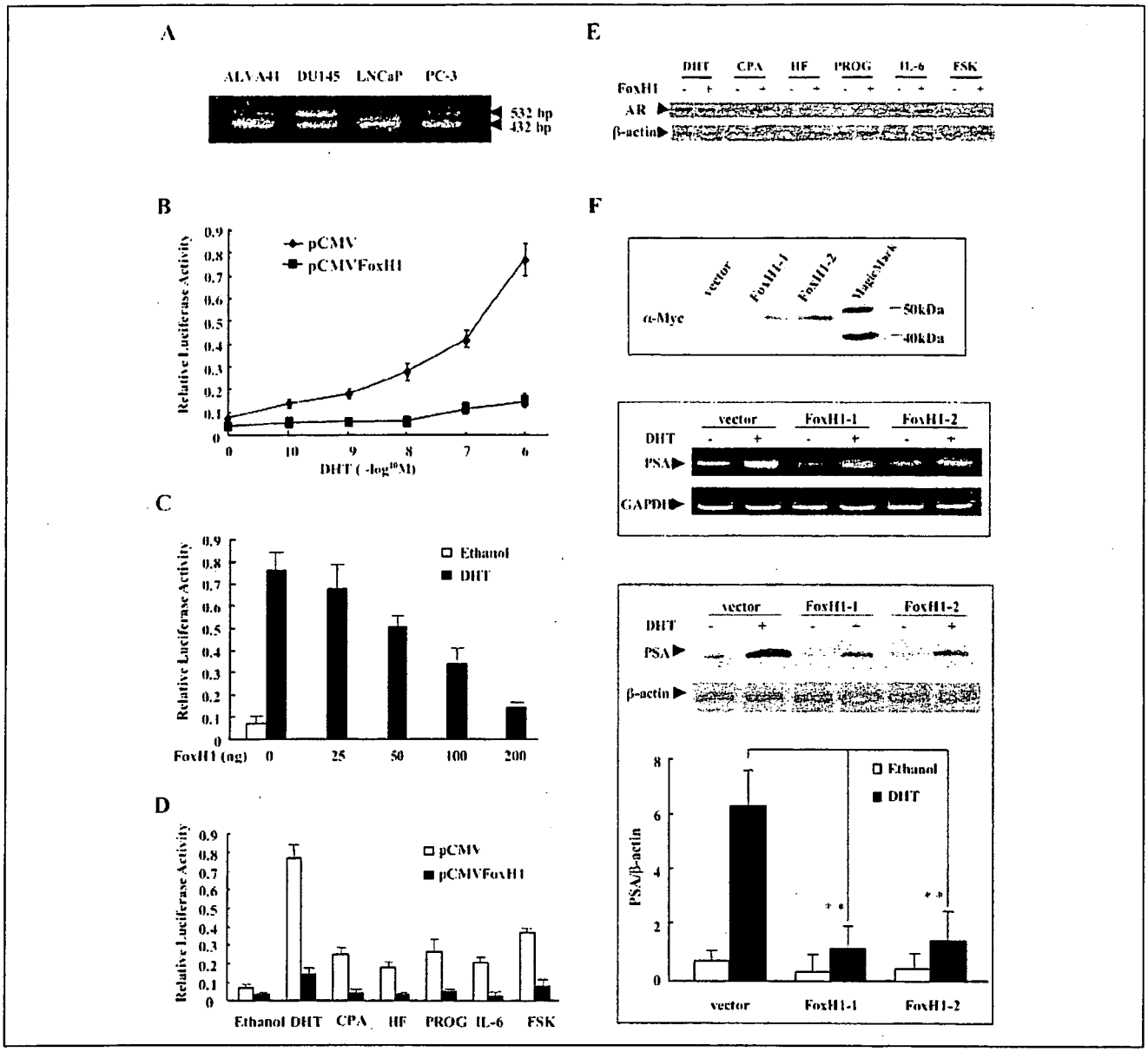

FIGURE 1. **Inhibitory effect of FoxH1 on AR transactivation in prostate cancer cells.** *A*, endogenous expression of FoxH1 in 4 prostate cancer cell lines. Total RNA was prepared from each prostate cancer cell line and subjected to RT-PCR as described under "Experimental Procedures." The cell lines examined are listed *above* the *panel*. *B–F*, inhibitory effects of FoxH1 on both ligand-dependent and -independent transactivation of the AR in LNCaP cells. *B–E*, LNCaP cells were transiently cotransfected with a DNA mixture containing 50 ng of pPSA-LUC, 1.5 ng of pRL-SV40, and increasing amounts (0–200 ng/well) (*C*) or 200 ng (*B* and *D*) of pCMVFoxH1 adjusted with the empty pCMV vector to produce equimolar amounts of the pCMV vector. The total amount of DNA in each well was brought to 250 ng with pBSK+ DNA. *B*, cells were treated with increasing concentrations of DHT as indicated. *C*, cells were exposed to 1 μM DHT. *D*, cells were exposed to the following concentrations of ligands: 1 μM DHT, 1 μM cyproterone acetate (*CPA*), 1 μM hydroxyflutamide (*HF*), 1 μM progesterone (*PROG*), 25 ng/ml interleukin-6 (*IL-6*), or 10 μM forskolin (*FSK*). *E*, AR expression in extracts (20 μg of protein) of LNCaP cells, corresponding to the same samples shown in *D*, were assessed by immunoblotting using the anti-AR antibody N-20 (1:500). The names of the samples are listed *above* the *panels*. *F*, pFoxH1-Myc was stably transfected into LNCaP cells, and the expression of FoxH1-Myc was investigated by immunoblotting (*top panel*). Endogenous PSA expression was also investigated by semiquantitative RT-PCR (*middle panel*) and immunoblotting (*bottom panel*) as described under "Experimental Procedures." Bands were measured by densitometry. Data are presented as the mean (±S.E.) ratio of PSA:β-actin proteins from three independent experiments (*bottom panel*). The blot shown in the figure shows the results of a typical experiment. **, $p < 0.01$. *GAPDH*, glyceraldehyde-3-phosphate dehydrogenase.

with 2 μg of the pCMVhAR or pCMV parent vector in 6-well plates using Lipofectamine (Invitrogen) according to the manufacturer's instructions. Transfected cells were cultured in the presence or absence of 10 nM DHT for 24 h and then harvested in celLytic™-M (Sigma) containing 1× Complete Mini-EDTA-free protease inhibitor mixture (Roche Applied Science). The protein concentration of each sample was measured and adjusted to 1 mg/ml. Next, an aliquot (160 μg) of each lysate was incubated with 3 μg of the anti-AR antibody C-19 (sc-815; Santa Cruz Biotechnology Inc.) or normal rabbit IgG as a control in TNE buffer (10 mM Tris-HCl, pH 7.8, 1% Nonidet P-40, 1 mM EDTA, 150 mM NaCl) containing 1× Complete Mini-EDTA-free protease inhibitor mixture and then further incubated with 25 μl of protein G magnetic beads (New England Biolabs Inc., Beverly, MA) at 4 °C for 2 h on a rotating platform. The beads were collected using a magnet, and the bound proteins were eluted in 1× SDS-PAGE sample buffer and subjected to 10% SDS-PAGE. A Western blot analysis was performed using the anti-Myc antibody (1:500) as described above, and the positive bands were detected using an enhanced chemiluminescence detection

system (Amersham Biosciences) and a VersaDoc™ imaging system (Bio-Rad).

Mammalian Two-hybrid Assays—Mammalian two-hybrid assays (Promega) were mainly performed according the manufacturer's protocol, with some modifications. NIH3T3 cells were transiently cotransfected with the indicated vectors in 24-well plates using the Superfect transfection reagent (Qiagen K. K.) in the presence or absence of 10 nM DHT. Luciferase activities were assayed as described above.

Statistical Analysis—Statistical significance was determined by one-factor analysis of variance followed by a post hoc test (Fisher's protected least significant difference test). $p < 0.05$ was considered statistically significant.

RESULTS

Expression of FoxH1 in Prostate Cancer Cell Lines—A previous study (39) reported that human FoxH1 gene expression was ubiquitous and could be detected in all normal human tissues tested as well as in several cancer cell lines. However, whether FoxH1 is expressed in LNCaP cells as well as in other prostate cancer lines has yet not been elucidated. Therefore, to investigate the role of FoxH1 in the cross-talk between activin A- and androgen-mediated signaling in prostate cancer, we initially used the primers described in the above-mentioned study (39) to investigate FoxH1 expression in the prostate cancer lines ALVA41, DU145, LNCaP, and PC-3 by RT-PCR. These primers spanned a 100-bp intron and discriminated between the spliced (423 bp) and unspliced (523 bp) products. As shown in Fig. 1*A*, a 423-bp band was detected in all 4 prostate cancer cell lines. Moreover, three of the cell lines also contained the unspliced product, which may arise from either genomic DNA or unprocessed transcripts.

FoxH1 Represses Both Ligand-dependent and -independent Transactivation of the AR in LNCaP Cells—Next, we examined the possible roles of FoxH1 expression in ligand-dependent and -independent transcription of the PSA promoter induced by endogenous AR by cotransfecting LNCaP cells, the most commonly used androgen-sensitive prostate cancer cell line, with a FoxH1 expression plasmid and a PSA-luciferase reporter gene. As shown in Fig. 1*B*, DHT activated the AR in a concentration-dependent manner, and an ~10-fold higher induction was observed in the presence of 1 μM DHT compared with vehicle treatment. Cotransfection of the FoxH1 expression plasmid brought about a marked repression of the DHT-induced AR activation at all concentrations of DHT tested (Fig. 1*B*), and the repression was dose-dependent (Fig. 1*C*). Furthermore, FoxH1 completely blocked the stimulatory effects of progesterone and the anti-androgens cyproterone acetate and hydroxyflutamide on the AR in LNCaP cells, which contains a mutation (T877A) that results in alterations of the specificity and sensitivity of the receptor to these molecules (50, 51) as well as the ligand-independent transactivation of the AR by interleukin-6 (52–54) and forskolin (55, 56) (Fig. 1*D*). In these and subsequent experiments, the inhibitory effect of FoxH1 on the AR transactivity was not due to a reduced AR expression level, since immunoblot analyses of extracts from the transfected cells revealed comparable amounts of immunoreactive protein (Fig. 1*E*). Together, these results demonstrate that FoxH1 represses both ligand-dependent and -independent transactivation of endogenous AR in LNCaP cells.

To further explore the relevance of FoxH1 in AR-mediated transactivation, we examined the relationship between FoxH1 expression and endogenous PSA expression in LNCaP cells. pFoxH1-Myc was stably transfected into LNCaP cells, and 2 isolated clones expressing similar protein levels of FoxH1-Myc, LNCaP/FoxH1-1, and LNCaP/FoxH1-2 were established (Fig. 1*F*, *top panel*) to investigate the effect of FoxH1 on

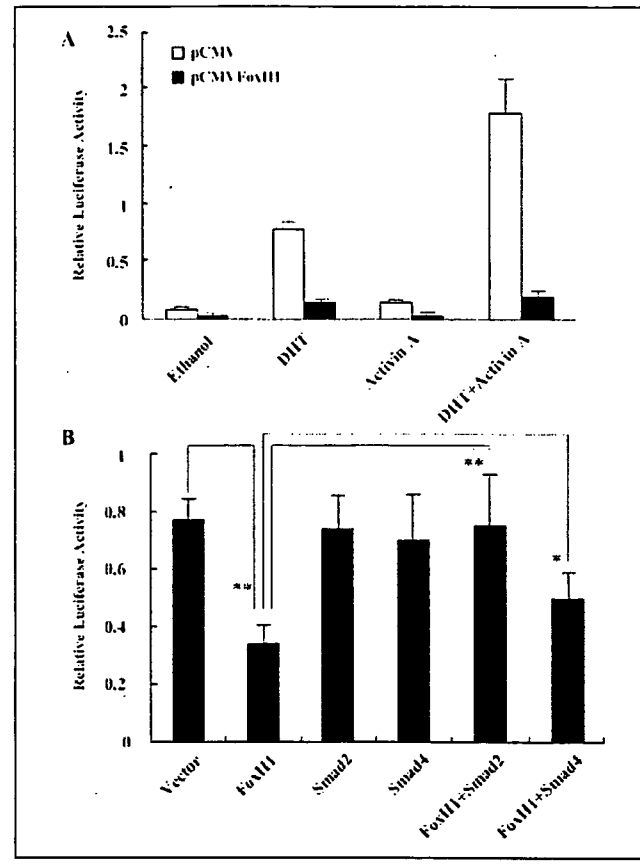

FIGURE 2. **Repression by FoxH1 is not rescued by activin A but is relieved by Smad2/4.** *A*, activin A has no effect on the FoxH1-mediated repression of PSA expression. LNCaP cells were cotransfected as described in the legend for Fig. 1, *C* and *D*, and then treated with 0.1% ethanol, 1 μM DHT, 25 ng/ml activin A, or DHT + activin A. *B*, LNCaP cells were cotransfected with 50 ng of pPSA-LUC and 1.5 ng of pRL-SV40 as well as 100 ng of pCMVFoxH1, 100 ng of a Smad expression vector alone, or 100 ng each of pCMVFoxH1 and a pcDNA3-Smad vector. The parent expression vectors were used to maintain equimolar concentrations across all cultures. After transfection, the cells were treated with 1 μM DHT. *, $p < 0.05$; **, $p < 0.01$.

PSA expression. As expected, stable expression of FoxH1 resulted in a parallel reduction of PSA expression in either mRNA or protein levels in both the absence and presence of DHT but had little effect on the levels of the housekeeping genes glyceraldehyde-3-phosphate dehydrogenase and β-actin (Fig. 1*F*, *middle* and *bottom panels*), indicating that FoxH1 could regulate the expression of endogenous androgen-responsive genes.

Repression of FoxH1 Is Not Rescued by Activin A but Is Relieved by Smad2/4 Proteins—Because FoxH1 mediates transcriptional responses to TGF-β/activin in a ligand-, receptor-, and Smad-dependent fashion (39)and activin A has been shown to induce PSA expression in LNCaP cells (26, 27, 41), we next investigated whether activin A and its effectors Smad2·Smad4 could alleviate the repression of the AR by FoxH1 in LNCaP cells. Consistent with previous reports, activin A induced transcription from the PSA promoter, and the PSA promoter induction after treatment with both DHT and activin A was additive compared with the values observed with either reagent alone (Fig. 2*A*). Unexpectedly, FoxH1 could still repress the AR-mediated transactivation of the PSA promoter in the presence of activin A, indicating that FoxH1-mediated inhibition was independent of activin A in LNCaP cells and that FoxH1 was dispensable for the stimulatory effect of activin A on PSA expression (26, 27, 41). On the other hand, in agreement with a previous report (57) neither Smad2 nor Smad4 alone had a signifi-

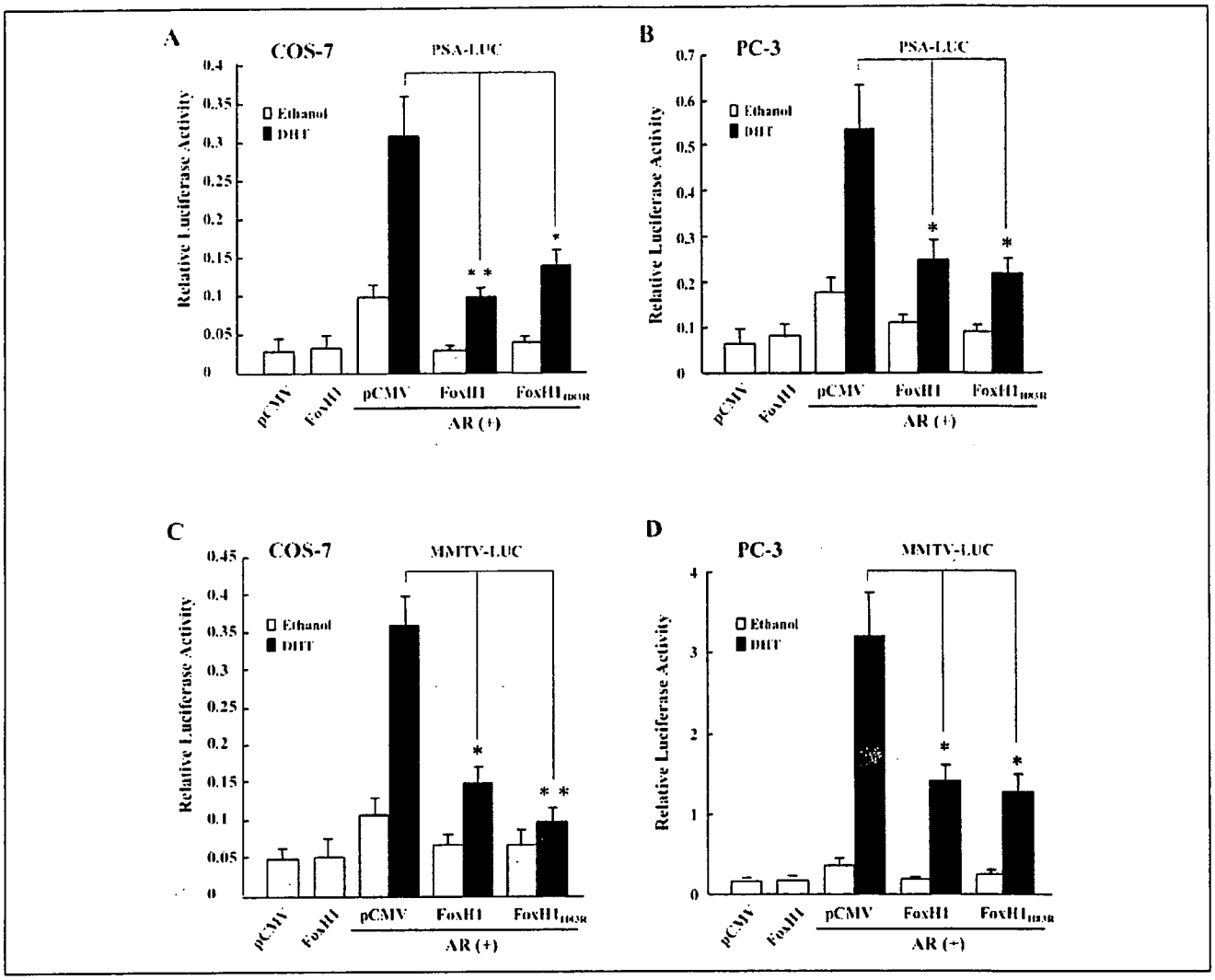

FIGURE 3. **Repression by FoxH1 is neither cell type- nor promoter context-dependent.** *A* and *B*, PSA-LUC reporter assays performed in COS-7 cells (*A*) or PC-3 cells (*B*). *C* and *D*, MMTV-LUC reporter assays performed in COS-7 cells (*C*) or PC-3 cells (*D*). The cells were cotransfected with 50 ng of pPSA-LUC or pMMTV-LUC, 1.5 ng of pRL-SV40, and 150 ng of pCMVFoxH1 or pCMVFoxH1$_{H83R}$ or an equimolar amount of the empty pCMV vector with or without 50 ng of a wild-type AR expression vector as indicated. After transfection, the cells were treated with 0.1% ethanol or 10 nM DHT. *, $p < 0.05$; **, $p < 0.01$.

cant effect on the AR-dependent transcription, whereas coexpression of Smad2 or Smad4 resulted in complete or partial relief of the repression by FoxH1, respectively (Fig. 2*B*). These results suggest that Smad2·Smad4 may be negative regulatory factors for the repression of the AR by FoxH1 through competition with the AR for binding to the limiting cellular FoxH1.

Repression of FoxH1 Is Neither Cell-type- Nor Promoter Context-dependent—To further explore the biological significance of the FoxH1-mediated repression, we examined the repression effect of FoxH1 on the wild-type AR in COS-7 and PC-3 cells using both pPSA-LUC and pMMTV-LUC as reporter genes. As shown in Fig. 3, FoxH1 as well as its mutant FoxH1$_{H83R}$, which has a mutation in the DNA binding Forkhead domain and completely lacks transcriptional activity (39), still significantly repressed AR-regulated transcription from either the PSA or MMTV promoter in both COS-7 and PC-3 cells. Notably, the basal transcription from the reporter genes was also reduced in the presence of FoxH1 but only in the presence of the AR (Fig. 3). In addition, the internal control *Renilla* luciferase activity was not influenced by FoxH1. Therefore, the repression by FoxH1 was specific for the AR and not a general transcriptional inhibition. These observations suggest that the inhibitory effect of FoxH1 on the AR is neither cell type- nor promoter context-dependent and is independent of its transactivity.

Selective Repression by FoxH1—Several of the corepressors identified to date, such as N-CoR and SMRT, can repress the transcriptional activity of other steroid hormone receptors as well as that of the AR (58–61). Therefore, it is important to investigate whether the repression by FoxH1 is specific for the AR or a more general phenomenon. To address this question, we tested GR, ER-α, ER-β, and PR isoforms in PC-3 cells under similar experimental conditions to those used for the AR. As shown in Fig. 4, these receptors showed ligand-dependent transactivation in the presence of their appropriate ligands, and cotransfection of FoxH1 resulted in obvious repressions of ER-α and ER-β as well as of the AR. In contrast, FoxH1 showed no significant repression of the transactivation of the GR and PR isoforms, demonstrating that the repression of the AR by FoxH1 did not result from competition with the AR for binding to the hormone response elements. In these experiments, the internal control *Renilla* luciferase activity was stable. Collectively, these results suggest that FoxH1 may be involved in multiple regulatory processes mediated by steroid hormone receptors.

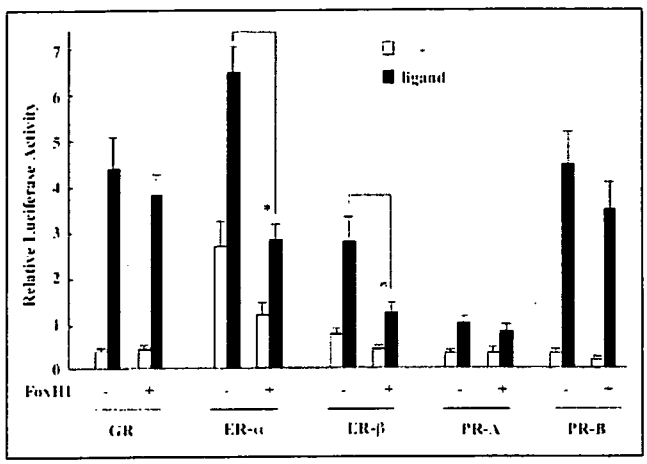

FIGURE 4. **Repression by FoxH1 is selective.** For each sample 50 ng of pMMTV-LUC or pERE2-tk109-LUC, 50 ng of the indicated corresponding steroid receptor expression constructs, and 1.5 ng of pRL-SV40 together with 150 ng of pCMVFoxH1 or an equimolar amount of the empty pCMV vector were cotransfected into PC-3 cells. After transfection the cells were treated with 10 nM concentrations of the specific ligand for each receptor. The ligands used were dexamethasone, 17β-estradiol, and progesterone. *, $p < 0.05$.

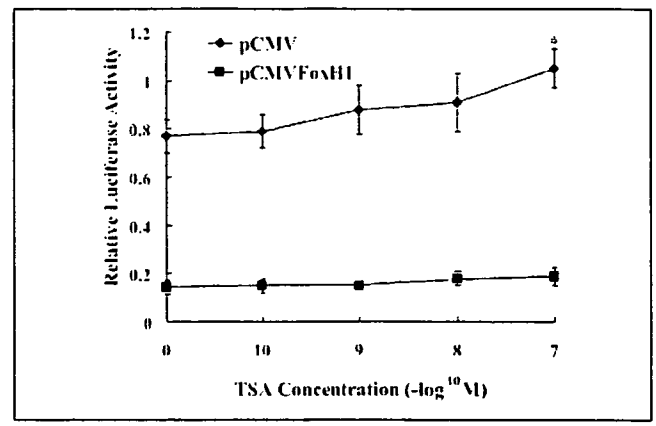

FIGURE 5. **Repression of the AR by FoxH1 does not require deacetylase activity.** LNCaP cells were cotransfected with 50 ng of pPSA-LUC, 1.5 ng of pRL-SV40, and 200 ng of pCMVFoxH1 or an equimolar amount of the empty pCMV vector. After transfection the cells were treated with 1 μM DHT alone or in combination with different concentrations of trichostatin A (*TSA*) as indicated. *, $p < 0.05$ *versus* the control.

Repression of the AR by FoxH1 Does Not Require Deacetylase Activity—Recent studies have shown that the transcriptional repression of the AR by some corepressors, such as TGIF (37) and ARR19 (62), is mediated through histone deacetylase pathways. In this regard, we examined whether trichostatin A (TSA), a specific inhibitor of histone deacetylase activity (63), had any influence on the repression of the AR by FoxH1 in LNCaP cells. Consistent with a previous report (64), treatment with 10^{-7} M TSA slightly increased the DHT-induced AR transactivity by about 30% (Fig. 5). However, TSA had no significant effect on the FoxH1-mediated inhibition at any of the doses tested, indicating that the repression of the AR by FoxH1 does not require deacetylase activity and that FoxH1 may repress AR-mediated transactivation through other mechanisms.

FoxH1 Abrogates Nuclear Foci Formation by the AR—We previously reported that DHT-bound AR formed foci in the nucleus, which were correlated with AR-mediated transactivations (44, 45). More recently, it was reported that the Tob-mediated suppression of AR activity may result from inhibition of the AR foci formation (65). Therefore, the prevention of AR foci formation may be responsible for the repression by FoxH1. To verify this hypothesis, we first examined the intracellular localization of the FoxH1 protein. As expected, the majority of FoxH1-GFP was homogeneously distributed in the nucleus in all the cell lines examined (Fig. 6, *A–C*). No significant changes were observed in the subcellular distribution of FoxH1-GFP before and after the addition of DHT or activin A. Consistent with our previous report (44), after cotransfection of LNCaP cells with pAR-GFP and the empty pCMV vector, the majority of AR-GFP was located homogeneously in the cytoplasm in untreated control cells (Fig. 6*D*), whereas treatment with 10 nM DHT resulted in nuclear translocation and fine foci formation by the AR in the nucleus (Fig. 6*E*). However, the addition of activin A (25 ng/ml) had little effect on the distribution of either unliganded or liganded AR (Fig. 6, *F* and *G*). In contrast, cotransfection with FoxH1 resulted in disruption of the DHT-induced foci formation, and AR-GFP was distributed homogeneously in the nucleus (Fig. 6*H*). In agreement with the transactivation assays, treatment with activin A did not recover the disruption of the DHT-induced foci formation by FoxH1 (Fig. 6*I*). Furthermore, replacement of pCMVFoxH1 by pCMVFoxH1$_{H83R}$ produced similar results (Fig. 6, *J* and *K*). Notably, and consistent with our previous report (45), CBP, a general integrator for nuclear receptors, was distributed in a mixed pattern with fine foci formation in a diffuse background in the nucleus (Fig. 6*L*). Cotransfection of FoxH1 had no obvious effect on the nuclear distribution of CBP (Fig. 6*M*), demonstrating that the disruption of foci formation by FoxH1 was specific for the AR rather than a general phenomenon.

FoxH1 Interacts Physically with AR—As a result of the above observations, we examined whether there was a physical interaction between the AR and FoxH1 using a coimmunoprecipitation analysis. pFoxH1-Myc was cotransfected into COS-7 cells with the empty pCMV vector or pCMVhAR. Cell extracts were immunoprecipitated with normal rabbit IgG (negative control) or an anti-AR antibody (C-19) followed by Western blotting with an anti-Myc monoclonal antibody. As shown in Fig. 7*A*, *upper panel*, FoxH1 protein was detected in anti-AR immunoprecipitates from cells cotransfected with the AR and FoxH1 in the absence or presence of 10 nM DHT but not in those from cells transfected with the AR or FoxH1 alone or when normal rabbit IgG was used. A similar result was obtained when pFoxH1-Myc was replaced by pFoxH1$_{H83R}$-Myc (Fig. 7*A*, *lower panel*). These data indicate that either FoxH1 or FoxH1$_{H83R}$ can form a specific complex with the AR.

Involvement of AF-1 in the Interaction of the AR with FoxH1—To further define the individual domains of the AR involved in binding to FoxH1, mammalian two-hybrid assays were carried out. The AR constructs consisted of amino acids 1–919 (pBIND-AR), amino acids 1–660 (pBIND-AR-NTD/DBD), and amino acids 615–919 (pBIND-AR-LBD) fused to the DBD of GAL4, whereas full-length FoxH1 was fused to the VP16 activation domain (pACT-FoxH1). As shown in Fig. 7*B*, the pG5-LUC reporter was induced after cotransfection of pBIND-AR-NTD/DBD and the empty pACT vector but not after cotransfection of the pBIND-AR-LBD construct, consistent with previous evidence that AF-1 in the NTD is responsible for most of the AR transactivation (66). Further induction was observed when pACT-FoxH1 was cotransfected with either pBIND-AR or pBIND-AR-NTD/DBD but not pBIND-AR-LBD. The addition of DHT (10 nM) further enhanced the transcription by about 2-fold in the case of pBIND-AR, whereas no significant induction was observed in the case of pBIND-AR-LBD. Moreover, pBIND-AR-NTD/DBD was found to have even stronger induction ability with FoxH1 than the full-length AR. Interestingly, when ANT-1, which specially enhances AR transactivation through a direct interaction with AR-AF-1 (46), was coexpressed, the induction of pG5-LUC by pACT-FoxH1 and pBIND-AR-NTD/DBD was completely blocked, suggesting that ANT-1 competed with FoxH1 for bind-

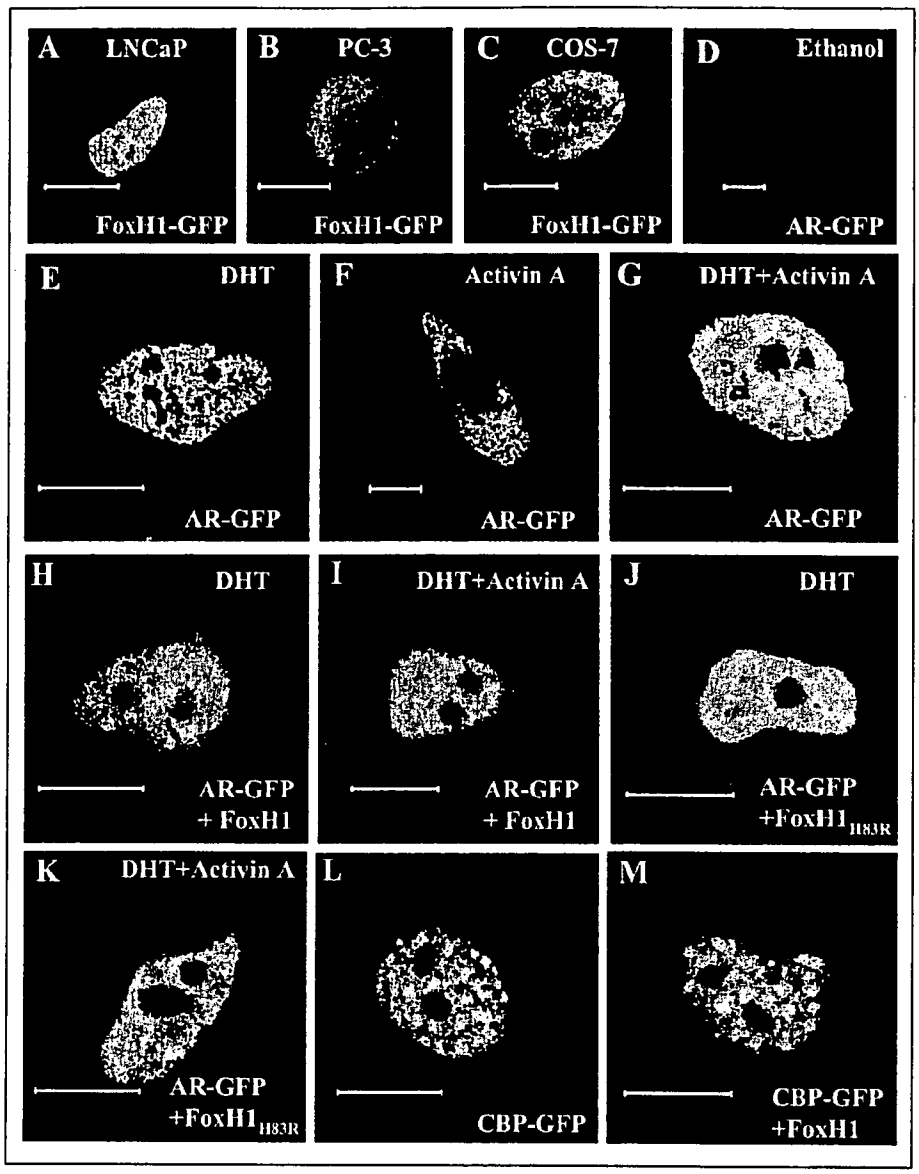

FIGURE 6. **Confocal laser microscopy images of FoxH1-GFP, AR-GFP, and CBP-GFP.** *A–C*, intracellular localizations of FoxH1 protein. pFoxH1-GFP was transiently transfected into LNCaP cells (*A*), PC-3 cells (*B*), and COS-7 cells (*C*), and the fluorescent signals in the cells were collected by confocal laser scanning microscopy. *D–M*, specific disruption of the AR nuclear foci formation by FoxH1. pAR-GFP or pCBP-GFP was cotransfected into LNCaP cells with the pCMV parent vector (*D–G* and *L*), pCMVFoxH1 (*H*, *I*, and *M*), or pCMVFoxH1$_{H83R}$ (*J* and *K*). After transfection the cells were treated with 0.1% ethanol (*D*), 10 nM DHT (*E*, *H*, and *J*), 25 ng/ml activin A (*F*), or DHT and activin A (*G*, *I*, and *K*) as indicated, and the fluorescent signals from AR-GFP or CBP-GFP were collected after 2 h. *Bars*, 10 μm.

ing to AR-AF-1. These data suggest that AF-1 may be involved in the interaction of the AR with FoxH1 in both the presence and absence of androgens.

FoxH1 Represses AR-AF-1 Function—Because our data implicated AF-1 as the site of FoxH1 corepressor activity, we investigated whether AF-1-dependent transactivation was sensitive to FoxH1 repression. As shown in Fig. 7*C*, when pBIND-AR-NTD (amino acids 1–532) was cotransfected together with pG5-LUC, there was a marked increase in the luciferase activity which was dramatically reduced when FoxH1 was coexpressed. These results provide additional evidence that AF-1 may be involved in the interaction between the AR and FoxH1 in cells.

DISCUSSION

To date many coregulators of the AR have been identified and characterized (13, 15). Compared with the coactivators, the AR corepressors identified are relatively fewer and less well characterized. The data obtained in the present study demonstrate a new function for FoxH1, which was expressed in LNCaP cells and the other prostate cancer cell lines tested, as a corepressor that attenuates the transactivation potential of the AR. This effect occurred in both the presence or absence of activin A, indicating that activin A was not involved in the repression of the AR by FoxH1 and, conversely, that FoxH1 was dispensable for the stimulatory effect of activin A on PSA expression (26, 27, 41). However, the possible roles of the FoxH1-mediated repression of the AR in activin signaling in prostate cancer require further investigation since Smad2/4 can rescue the repression of the AR by FoxH1, and a mutually antagonistic interaction between activin and androgen signaling has been shown to be involved in modulating the expressions of cell cycle regulatory proteins such as Rb, E2F-1, and p27 (27), thereby playing an important role in the regulation of prostate cancer cell growth. Hence, further clarification of the effect of the FoxH1-mediated repression of the AR on the expressions of these cell cycle regulatory proteins would help to elucidate the molecular mechanism through which activin A regulates gene expression and growth in the prostate.

The AR shares hormone response element sequences in the DNA with GR and PR (67). In this regard, the NH_2-terminal region, which varies among these receptors, is considered to be responsible for the cell- and ligand-specific regulation of their target genes (66, 68, 69). The

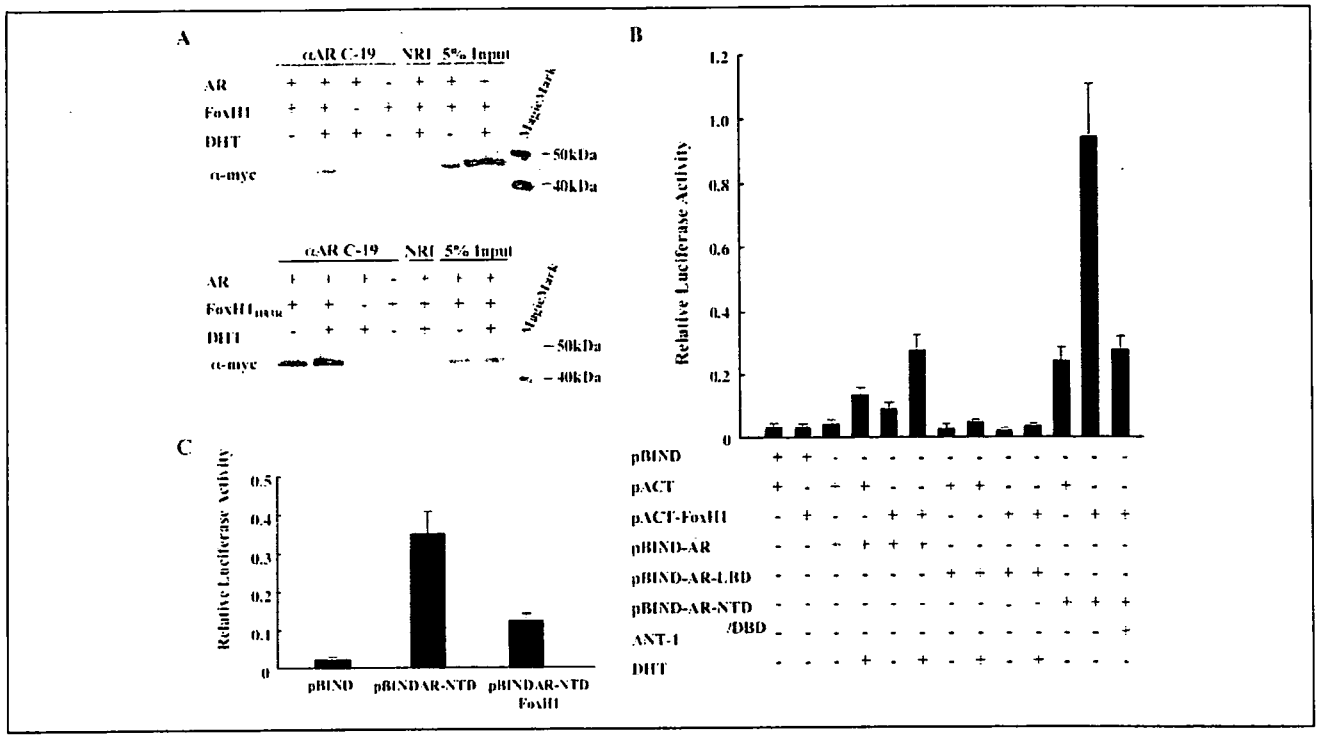

FIGURE 7. **Physical interaction between FoxH1 and the AR.** *A*, coimmunoprecipitation of the AR with FoxH1 or FoxH1H83R was performed as described under "Experimental Procedures." Whole cell extracts were immunoprecipitated with an anti-AR antibody (*C-19*) or normal rabbit IgG (*NRI*), and the immunoprecipitated fractions were analyzed by immunoblotting with an anti-Myc antibody. *B*, involvement of AF-1 in the interaction of the AR with FoxH1. Mammalian two-hybrid assays were carried out to test for an *in vivo* interaction between the AR and FoxH1. NIH3T3 cells were cotransfected with a DNA mixture containing 100 ng of pG5-LUC, 1.5 ng of pRL-SV40, 75 ng of pACT-FoxH1, or an equimolar amount of the pACT parent vector, 25 ng of pBIND-AR or equimolar amounts of pBIND-AR-NTD/DBD, pBIND-AR-LBD or the pBIND parent vector, and 225 ng of pcDNA3-ANT-1 or an equimolar amount of the pcDNA3 parent vector. The total DNA was adjusted to 600 ng/well with pBSK+ DNA. After transfection the cells were treated with 0.1% ethanol or 10 nM DHT. *C*, FoxH1 represses AR-AF-1 function. NIH3T3 cells were cotransfected with 100 ng of pG5-LUC, 1.5 ng of pRL-SV40, 50 ng of pCMV-FoxH1, or an equimolar amount of pCMV parent vector and 10 ng of pBIND-AR-NTD or an equimolar amount of the pBIND parent vector. The total DNA was adjusted to 600 ng/well with pBSK+ DNA. Approximately 24 h after transfection the cells were harvested, and the luciferase activity was measured.

AR is thought to be quite unique among the nuclear receptor superfamily members, since most if not all of its activities are mediated via the ligand-independent constitutive activity of the AF-1 (66). The fundamental role of the AR-AF-1 was further supported by our recent finding (43) that the absence of an AR-AF-1-specific coactivator resulted in androgen insensitivity syndrome. Our current observations show that AF-1 is involved in the interaction of the AR with FoxH1, which may explain why the inhibitory effect of FoxH1 on steroid receptors is selective. Because FoxH1 is expressed in mammary gland tissue (39), it is of interest to further elucidate whether FoxH1 is also able to interact with ER in breast cancer cell lines, such as MCF-7, and whether it is involved in the regulation of TGF-β/activin signaling during the growth of breast cancer.

In addition to SRC-1 (70) and CBP/P300 (71), which interact with both AF-1 and AF-2 of the AR, many coregulators, such as Hey1 (72), SMRT (60), SMAD3 (57), AES (73), cyclin D1 (74), ANT-1 (46), ARA24 (75), and ARA160 (76), have also been shown to interact preferentially with the AF-1. Interestingly, STAT3, a critical signaling molecule required for ligand-independent transactivation of the AR by interleukin-6, also associates with the AR via AF-1 (53, 77, 78). Because androgen levels do not fluctuate dramatically in adult males, the relative levels of coactivators *versus* corepressors binding to the AR may play a critical role in modulating AR function (15, 79). Indeed, Hey1 (72) and SMRT (60) have been shown to attenuate AR transcriptional activity through interrupting the interaction between the AR and SRC-1. Similarly, we demonstrated that ANT-1 competed with FoxH1 for binding to the AR. Therefore, interrupting the interactions between the AR and its coactivators may be responsible for the inhibitory effects of FoxH1 on the ligand-dependent and -independent transactivation of the AR. In addition, FoxH1, as well as Hey1, could attenuate the AR transactivation potential in both the presence and absence of androgens, suggesting that therapeutic interventions based on AR-coregulator interactions could be designed to block both androgen-dependent and -independent growth of tumor cells.

We previously reported a sensitive confocal laser microscopy approach that can clearly distinguish the transcriptionally active and inactive forms of the AR *in vivo* (44). More recently, we reported that transfer to common compartments (foci) of the nucleus and complex formation with coactivators, such as SRC-1, TIF2, and CBP, may be essential processes for eliciting the transactivation function of the AR (45). In the present study we observed that FoxH1 had no effect on the nuclear translocation of the AR but specifically blocked the DHT-induced foci formation by the AR in LNCaP cells. Therefore, the simplest explanation for our current finding that FoxH1 represses the AR-mediated transactivation is that FoxH1 maybe compete with AR coactivators, such as SRC-1 and ANT-1, for binding to the AR, thereby inhibiting the formation of the transcriptionally active complex. However, further studies are required to elucidate the precise mechanism of the FoxH1-induced repression of AR-mediated transactivation. Moreover, it will be interesting to investigate whether disruption of the foci formation is also involved in the repression of AR-mediated transactivation by other corepressors, such as Hey1 and SMRT.

In conclusion, this is the first report to demonstrate that association of FoxH1 with the AR can inhibit the transactivation potential of the AR.

Further studies of the expression of FoxH1 in prostate cancer at different stages and its role in the mutually antagonistic effects of androgen and activin A will provide fresh insights into the biology of prostate cancer and may lead to the development of new treatments.

Acknowledgments—We thank Drs. Bert Vogelstein, Shigeaki Kato, Jer-Tsong Hsieh, and Pierre Chambon for the kind gifts of plasmids.

REFERENCES

1. Santos, A. F., Huang, H., and Tindall, D. J. (2004) *Steroids* 69, 79–85
2. Taplin, M. E., and Balk, S. P. (2004) *J. Cell. Biochem.* 91, 483–490
3. Culig, Z. (2003) *Urology* 62, Suppl. 5A, 21–26
4. Navarro, D., Luzardo, O. P., Fernandez, L., Chesa, N., and Diaz-Chico, B. N. (2002) *J. Steroid Biochem. Mol. Biol.* 81, 191–201
5. Lee, E. C., and Tenniswood, M. P. (2004) *J. Cell. Biochem.* 91, 662–670
6. Zhou, J., Scholes, J., and Hsieh, J. T. (2001) *Cancer Metastasis Rev.* 20, 351–362
7. Huang, H., and Tindall, D. J. (2002) *Crit. Rev. Eukaryotic Gene Expression* 12, 193–207
8. Dehm, S. M., and Tindall, D. J. (2005) *Expert Rev. Anticancer Ther.* 5, 63–74
9. Lee, H. J., and Chang, C. (2003) *Cell. Mol. Life Sci.* 60, 1613–1622
10. Haendler, B. (2002) *Biomed. Pharmacother.* 56, 78–83
11. Slagsvold, T., Kraus, I., Bentzen, T., Palvimo, J., and Saatcioglu, F. (2000) *Mol. Endocrinol.* 14, 1603–1617
12. Brinkmann, A. O., Blok, L. J., de Ruiter, P. E., Doesburg, P., Steketee, K., Berrevoets, C. A., and Trapman, J. (1999) *J. Steroid Biochem. Mol. Biol.* 69, 307–313
13. Heinlein, C. A., and Chang, C. (2002) *Endocr. Rev.* 23, 175–200
14. Shang, Y., Myers, M., and Brown, M. (2002) *Mol. Cell* 9, 601–610
15. Wang, L., Hsu, C. L., and Chang, C. (2005) *Prostate* 63, 117–130
16. Ying, S. Y. (1989) *J. Steroid Biochem.* 33, 705–713
17. Ying, S. Y., Zhang, Z., Furst, B., Batres, Y., Huang, G., and Li, G. (1997) *Proc. Soc. Exp. Biol. Med.* 214, 114–122
18. Chen, Y. G., Lui, H. M., Lin, S. L., Lee, J. M., and Ying, S. Y. (2002) *Exp. Biol. Med.* 227, 75–87
19. van Schaik, R. H., Wierikx, C. D., Timmerman, M. A., Oomen, M. H., van Weerden, W. M., van der Kwast, T. H., van Steenbrugge, G. J., and de Jong, F. H. (2000) *Br. J. Cancer* 82, 112–117
20. McPherson, S. J., Mellor, S. L., Wang, H., Evans, L. W., Groome, N. P., and Risbridger, G. P. (1999) *Endocrinology* 140, 5303–5309
21. Mellor, S. L., Cranfield, M., Ries, R., Pedersen, J., Cancilla, B., de Kretser, D., Groome, N. P., Mason, A. J., and Risbridger, G. P. (2000) *J. Clin. Endocrinol. Metab.* 85, 4851–4858
22. Thomas, T. Z., Chapman, S. M., Hong, W., Gurusingfhe, C., Mellor, S. L., Fletcher, R., Pedersen, J., and Risbridger, G. P. (1998) *Prostate* 34, 34–43
23. Dalkin, A. C., Gilrain, J. T., Bradshaw, D., and Myers, C. E. (1996) *Endocrinology* 137, 5230–5235
24. McPherson, S. J., Thomas, T. Z., Wang, H., Gurusinghe, C. J., and Risbridger, G. P. (1997) *J. Endocrinol.* 154, 535–545
25. Wang, Q. F., Tilly, K. I., Tilly, J. L., Preffer, F., Schneyer, A. L., Crowley, W. F., Jr., and Sluss, P. M. (1996) *Endocrinology* 137, 5476–5483
26. Zhang, Z., Zhao, Y., Batres, Y., Lin, M. F., and Ying, S. Y. (1997) *Biochem. Biophys. Res. Commun.* 234, 362–365
27. Carey, J. L., Sasur, L. M., Kawakubo, H., Gupta, V., Christian, B., Bailey, P. M., and Maheswaran, S. (2004) *Mol. Endocrinol.* 18, 696–707
28. Baker, J. C., and Harland, R. M. (1997) *Curr. Opin. Genet. Dev.* 7, 467–473
29. Abe, Y., Minegishi, T., and Leung, P. C. (2004) *Growth Factors* 22, 105–110
30. Liberati, N. T., Datto, M. B., Frederick, J. P., Shen, X., Wong, C., Rougier-Chapman, E. M., and Wang, X. F. (1999) *Proc. Natl. Acad. Sci. U. S. A.* 96, 4844–4849
31. Janknecht, R., Wells, N. J., and Hunter, T. (1998) *Genes Dev.* 12, 2114–2119
32. Feng, X. H., Zhang, Y., Wu, R. Y., and Derynck, R. (1998) *Genes Dev.* 12, 2153–2163
33. Wotton, D., Lo, R. S., Lee, S., and Massague, J. (1999) *Cell* 97, 29–39
34. Fronsdal, K., Engedal, N., Slagsvold, T., and Saatcioglu, F. (1998) *J. Biol. Chem.* 273, 31853–31859
35. Sato, N., Sadar, M. D., Bruchovsky, N., Saatcioglu, F., Rennie, P. S., Sato, S., Lange, P. H., and Gleave, M. E. (1997) *J. Biol. Chem.* 272, 17485–17494
36. Fu, M., Wang, C., Reutens, A. T., Wang, J., Angeletti, R. H., Siconolfi-Baez, L., Ogryzko, V., Avantaggiati, M. L., and Pestell, R. G. (2000) *J. Biol. Chem.* 275, 20853–20860
37. Sharma, M., and Sun, Z. (2001) *Mol. Endocrinol.* 15, 1918–1928
38. Liu, B., Dou, C. L., Prabhu, L., and Lai, E. (1999) *Mol. Cell. Biol.* 19, 424–430
39. Zhou, S., Zawel, L., Lengauer, C., Kinzler, K. W., and Vogelstein, B. (1998) *Mol. Cell* 2, 121–127
40. Chen, X., Weisberg, E., Fridmacher, V., Watanabe, M., Naco, G., and Whitman, M. (1997) *Nature* 389, 85–89
41. Fujii, Y., Kawakami, S., Okada, Y., Kageyama, Y., and Kihara, K. (2004) *Am. J. Physiol. Endocrinol. Metab.* 286, 927–931
42. Nakao, R., Haji, M., Yanase, T., Ogo, A., Takayanagi, R., Katsube, T., Fukumaki, Y., and Nawata, H. (1992) *J. Clin. Endocrinol. Metab.* 74, 1152–1157
43. Adachi, M., Takayanagi, R., Tomura, A., Imasaki, K., Kato, S., Goto, K., Yanase, T., Ikuyama, S., and Nawata, H. (2000) *N. Engl. J. Med.* 343, 856–862
44. Tomura, A., Goto, K., Morinaga, H., Nomura, M., Okabe, T., Yanase, T., Takayanagi, R., and Nawata, H. (2001) *J. Biol. Chem.* 276, 28395–28401
45. Saitoh, M., Takayanagi, R., Goto, K., Fukamizu, A., Tomura, A., Yanase, T., and Nawata, H. (2002) *Mol. Endocrinol.* 16, 694–706
46. Zhao, Y., Goto, K., Saitoh, M., Yanase, T., Nomura, M., Okabe, T., Takayanagi, R., and Nawata, H. (2002) *J. Biol. Chem.* 277, 30031–30039
47. Mukasa, C., Nomura, M., Tanaka, T., Tanaka, K., Nishi, Y., Okabe, T., Goto, K., Yanase, T., and Nawata, H. (2003) *Endocrinology* 144, 1603–1611
48. Chen, C. D., Welsbie, D. S., Tran, C., Baek, S. H., Chen, R., Vessella, R., Rosenfeld, M. G., and Sawyers, C. L. (2004) *Nat. Med.* 10, 33–39
49. Lau, K. M., LaSpina, M., Long, J., and Ho, S. M. (2000) *Cancer Res.* 60, 3175–3182
50. Kokontis, J., Ito, K., Hiipakka, R. A., and Liao, S. (1991) *Receptor* 1, 271–279
51. Veldscholte, J., Ris-Stalpers, C., Kuiper, G. G., Jenster, G., Berrevoets, C., Claassen, E., van Rooij, H. C., Trapman, J., Brinkmann, A. O., and Mulder, E. (1990) *Biochem. Biophys. Res. Commun.* 173, 534–540
52. Ueda, T., Bruchovsky, N., and Sadar, M. D. (2002) *J. Biol. Chem.* 277, 7076–7085
53. Chen, T., Wang, L. H., and Farrar, W. L. (2000) *Cancer Res.* 60, 2132–2135
54. Hobisch, A., Eder, I. E., Putz, T., Horninger, W., Bartsch, G., Klocker, H., and Culig, Z. (1998) *Cancer Res.* 58, 4640–4645
55. Kim, J., Jia, L., Stallcup, M. R., and Coetzee, G. A. (2005) *J. Mol. Endocrinol.* 34, 107–118
56. Sadar, M. D. (1999) *J. Biol. Chem.* 274, 7777–7783
57. Hayes, S. A., Zarnegar, M., Sharma, M., Yang, F., Peehl, D. M., ten Dijke, P., and Sun, Z. (2001) *Cancer Res.* 61, 2112–2118
58. Ordentlich, P., Downes, M., and Evans, R. M. (2001) *Curr. Top. Microbiol. Immunol.* 254, 101–116
59. Privalsky, M. L. (2001) *Curr. Top Microbiol. Immunol.* 254, 117–136
60. Dotzlaw, H., Moehren, U., Mink, S., Cato, A. C., Iniguez Lluhi, J. A., and Baniahmad, A. (2002) *Mol. Endocrinol.* 16, 661–673
61. Berrevoets, C. A., Umar, A., Trapman, J., and Brinkmann, A. O. (2004) *Biochem. J.* 379, 731–738
62. Jeong, B. C., Hong, C. Y., Chattopadhyay, S., Park, J. H., Gong, E. Y., Kim, H. J., Chun, S. Y., and Lee, K. (2004) *Mol. Endocrinol.* 18, 13–25
63. Taunton, J., Hassig, C. A., and Schreiber, S. L. (1996) *Science* 272, 408–411
64. Jia, L., Choong, C. S., Ricciardelli, C., Kim, J., Tilley, W. D., and Coetzee, G. A. (2004) *Cancer Res.* 64, 2619–2626
65. Kawate, H., Wu, Y., Ohnaka, K., Nawata, H., and Takayanagi, R. (2005) *Mol. Cell. Endocrinol.* 230, 77–86
66. McEwan, I. J. (2004) *Endocr. Relat. Cancer* 11, 281–293
67. Quigley, C. A., De Bellis, A., Marschke, K. B., el-Awady, M. K., Wilson, E. M., and French, F. S. (1995) *Endocr. Rev.* 16, 271–321
68. Tora, L., Gronemeyer, H., Turcotte, B., Gaub, M. P., and Chambon, P. (1988) *Nature* 333, 185–188
69. Warnmark, A., Treuter, E., Wright, A. P., and Gustafsson, J. A. (2003) *Mol. Endocrinol.* 17, 1901–1909
70. Bevan, C. L., Hoare, S., Claessens, F., Heery, D. M., and Parker, M. G. (1999) *Mol. Cell. Biol.* 19, 8383–8392
71. Ogryzko, V. V., Schiltz, R. L., Russanova, V., Howard, B. H., and Nakatani, Y. (1996) *Cell* 87, 953–959
72. Belandia, B., Powell, S. M., Garcia-Pedrero, J. M., Walker, M. M., Bevan, C. L., and Parker, M. G. (2005) *Mol. Cell. Biol.* 25, 1425–1436
73. Yu, X., Li, P., Roeder, R. G., and Wang, Z. (2001) *Mol. Cell. Biol.* 21, 4614–4625
74. Petre, C. E., Wetherill, Y. B., Danielsen, M., and Knudsen, K. E. (2002) *J. Biol. Chem.* 277, 2207–2215
75. Hsiao, P. W., Lin, D. L., Nakao, R., and Chang, C. (1999) *J. Biol. Chem.* 274, 20229–20234
76. Hsiao, P. W., and Chang, C. (1999) *J. Biol. Chem.* 274, 22373–22379
77. Matsuda, T., Junicho, A., Yamamoto, T., Kishi, H., Korkmaz, K., Saatcioglu, F., Fuse, H., and Muraguchi, A. (2001) *Biochem. Biophys. Res. Commun.* 283, 179–187
78. Lou, W., Ni, Z., Dyer, K., Tweardy, D. J., and Gao, A. C. (2000) *Prostate* 42, 239–242
79. Dotzlaw, H., Papaioannou, M., Moehren, U., Claessens, F., and Baniahmad, A. (2003) *Mol. Cell. Endocrinol.* 213, 79–85

Available online at www.sciencedirect.com
SCIENCE DIRECT
ELSEVIER
Biochemical and Biophysical Research Communications 341 (2006) 192–201
BBRC
www.elsevier.com/locate/ybbrc

Identification of the functional domains of ANT-1, a novel coactivator of the androgen receptor ☆

Shuli Fan, Kiminobu Goto [1], Guangchun Chen, Hidetaka Morinaga, Masatoshi Nomura, Taijiro Okabe, Hajime Nawata, Toshihiko Yanase *

Department of Medicine and Bioregulatory Science (3rd Department of Internal Medicine), Graduate School of Medical Sciences, Kyushu University, Maidashi 3-1-1, Higashi-ku, Fukuoka 812-8582, Japan

Received 29 November 2005
Available online 9 January 2006

Abstract

Previously, we identified a transcriptional coactivator for the activation function-1 (AF-1) domain of the human androgen receptor (AR) and designated it androgen receptor N-terminal domain transactivating protein-1 (ANT-1). This coactivator, which contains multiple tetratricopeptide repeat (TPR) motifs from amino acid (aa) 294, is identical to a component of U5 small nuclear ribonucleoprotein particles and binds specifically to the AR or glucocorticoid receptor. Here, we identified four distinct functional domains. The AR-AF-1-binding domain, which bound to either aa 180–360 or 360–532 in AR-AF-1, clearly overlapped with TAU-1 and TAU-5. This domain and the subnuclear speckle formation domain in ANT-1 were assigned within the TPR motifs, while the transactivating and nuclear localization signal domains resided within the N-terminal sequence. The existence of these functional domains may further support the idea that ANT-1 can function as an AR-AF-1-specific coactivator while mediating a transcription-splicing coupling.

Keywords: Androgen receptor; Activation function-1; Nuclear localization signal; Small nuclear ribonucleoprotein particle; Splicing factor compartment; Tetratricopeptide repeat; Transcriptional coactivator

The androgen receptor (AR) harbors two transcription activation function (AF) domains: the constitutively active AF-1 located in the N-terminal transactivating domain and the ligand-dependent AF-2 within the C-terminal ligand-binding domain [1]. The AR is considered to be quite unique among the members of the nuclear receptor superfamily, because most, if not all, of its activities are mediated via the ligand-independent constitutive activity of AF-1 [2,3]. This is in strong contrast to estrogen receptor α (ER α), in which the overall transactivation capacities are primarily dependent on AF-2 [4]. The AR shares hormone response element sequences on the DNA with the receptors for glucocorticoids (GR), mineralocorticoids, and progesterone [5]. In this regard, the N-terminal domain (NTD), which varies among these receptors, is thought to be responsible for the cell- and ligand-specific regulation of their target genes [6]. The fundamental role of AR-AF-1 was further supported by our clinical finding that the absence of an AR-AF-1-specific transcription coactivator results in androgen insensitivity syndrome [7]. To date, in addition to p300/CBP, SRC-1 and caveolin-1, which interact with both AF-1 and AF-2 [2,8,9], almost 20 proteins have been proposed to bind to the AR N-terminal transactivating domain, including basal transcription factors such as TFIIF [10], co-repressors [11–13], and

☆ *Abbreviations:* aa, amino acid(s); AF, activation function; ANT-1, androgen receptor N-terminal domain-binding protein-1; AR, androgen receptor; DHT, dihydrotestosterone; ER, estrogen receptor; GR, glucocorticoid receptor; NLS, nuclear localization signal; NTD, N-terminal domain; SFC, splicing factor compartment; snRNP, small nuclear ribonucleoprotein particle; TPR, tetratricopeptide repeat.

* Corresponding author. Fax: +81 92 642 5297.
E-mail address: yanase@intmed3.med.kyushu-u.ac.jp (T. Yanase).
[1] Present address: Internal Medicine and the Elderly Care, Kasamatsukai Medical Corporation Ariyoshi Hospital, Oo-aza Kamiariki 397-1, Miyata, Kurate-gun County, Fukuoka 823-0015, Japan.

0006-291X/$ - see front matter © 2005 Elsevier Inc. All rights reserved.
doi:10.1016/j.bbrc.2005.12.167

coactivators [14,15] as well as other unique proteins, including cyclin E [16], breast cancer susceptibility gene 1 (*BRCA1*) [17], and the RNA molecule SRA [18].

We previously isolated a cDNA sequence encoding a novel coactivator for the AR [19]. This protein, designated AR NTD transactivating protein-1 (ANT-1), bound to the AF-1 of the AR and GR, but not that of ER α, and specifically enhanced the AR- and GR-AF-1 transactivation capacities in a ligand-independent manner. The amino acid sequence of ANT-1 was identical to that of the PRP6 protein [20,21], a mammalian homolog of yeast prp6p, which forms U5 small nuclear ribonucleoprotein particles (snRNPs) involved in the spliceosome. In addition to ANT-1, cyclin E [22] and $p54^{nrb}$ [23], another AR-AF-1-binding protein, are also known to interact with splicing factors, suggesting that AR-AF-1 may be involved in the pre-mRNA splicing machinery. Upon confocal microscopic image analysis, ANT-1 was compartmentalized into 20–40 coarse splicing factor compartment (SFC) speckles against a background of diffuse reticular distribution [19]. Interestingly, the ANT-1 sequence shows structural significance, since it contains 19 copies of the tetratricopeptide repeat (TPR) motif, which plays significant roles in protein–protein interactions [24], in the final two-thirds of the C-terminal region.

It has been hypothesized that active gene transcription may occur simultaneously with pre-mRNA processing, and this process has been designated co-transcriptional splicing or "transcription-splicing coupling" [25,26]. Furthermore, steroid hormones affect the processing of pre-mRNA synthesized from steroid-sensitive promoters, but not from steroid-unresponsive promoters [27]. The nucleus contains different sets of functional compartments, often called "speckles," which include SFCs showing nearly 20–50 large speckles [28]. After three-dimensional reconstruction of confocal microscopic images, we observed that the activated AR forms 200–400 fine speckles that chiefly recruit AF-2-interacting transcriptional cofactors [29,30]. These speckles are mostly located in euchromatin regions and merge with the diffuse distribution of ANT-1. In contrast to cytoplasmic compartments, the subnuclear compartments are not sequestered by membrane structures, thereby allowing rapid movement of the protein components across the compartment. Therefore, interaction of ANT-1 with the AR or GR in the diffuse distribution of ANT-1 may play a role in the interaction between these two distinct subnuclear compartments. We speculated that it should contain at least four functional domains, namely a nuclear localization signal (NLS) domain, a transactivating domain, a speckle formation domain, and an AR-AF-1-binding domain. Therefore, in the present study, we performed analyses to investigate the presence of these functional domains in ANT-1.

Materials and methods

Cell culture. COS-7 cells and NIH3T3 fibroblast cells were maintained in Dulbecco's modified Eagle's medium supplemented with 10% fetal calf serum. To establish cells (designated COS-AR-AF-1 cells) that stably expressed AR-AF-1 (amino acids (aa) 1–532), COS-7 cells in 10 cm dishes were transfected with 5 μg of an AR-AF-1 expression plasmid [7] using the Superfect Transfection Reagent (Qiagen) according to the manufacturer's instructions. An initial selection was performed with 1 μg/ml of puromycin (Sigma) at 24 h after the transfection, and the selected cells were subsequently grown in bulk culture for 5–6 days. A single clone was isolated by limited dilution and then cultured for a further 2 weeks. The presence of the AR-AF-1 fragment in the stably transfected line was monitored by Western blotting using an anti-AR N-20 antibody (Santa Cruz Biotechnology).

Plasmids and site-directed mutagenesis. pMMTV-luc, containing the luciferase gene driven by the mouse mammary tumor virus long terminal repeat harboring a hormone response element for both the AR and GR, and the plasmids expressing ANT-N and ANT-C were described previously [7,19]. The expression plasmid for human ER α (pSG5-ER α) and a reporter plasmid for ER α (pERE2-tk109-luc) were provided by Dr. Shigeaki Kato (University of Tokyo, Tokyo, Japan). pANT-1-myc expressing myc-tagged full-length ANT-1 was prepared as described previously [19], and plasmids expressing truncated mutants of myc-tagged ANT-1 were obtained by appropriate restriction enzyme digestion or PCR amplification. Briefly, ΔANT(290) was obtained by restriction digestion with *Kpn*I and *Eco*RV. For ΔANT(146), ΔANT(172), ΔANT(399), ΔANT(499), and ΔANT(173–499) PCR was initially performed to create DNA fragments that contained a *Kpn*I restriction site at the 5′ end and an *Xba*I restriction site at the 3′ end. These fragments were then digested with *Kpn*I and *Xba*I, and subcloned into appropriate expression plasmids such as pcDNA3, pcDNA3-myc-his or pEGFP.

We used the Check Mate Mammalian Two-Hybrid System (Promega), in which the GAL-4 DNA-binding domain is present in a pBind plasmid, the herpes simplex virus VP16 activation domain is present in a pACT plasmid, and five GAL-4-binding sequences and a luciferase gene are present in the pG5luc plasmid. Truncated fragments of ANT-1 with an *Xba*I restriction site at the 5′ end and a *Kpn*I site at the 3′ end were obtained by PCR amplification and then subcloned into pACT to generate VP-ΔANT(146), VP-ΔANT(172), VP-ΔANT(290), VP-ΔANT(399), VP-ΔANT(499), and VP-ANT-C. Truncated fragments of the AR-NTD with a *Bam*HI restriction site at the 5′ end and an *Xba*I site at the 3′ end were also obtained by PCR amplification and then subcloned into pBind plasmids to generate GAL-AR(1–180), GAL-AR(180–360), GAL-AR(360–520), and GAL-AR(1–660).

Site-directed mutagenesis was performed using a Quick Change Site-directed Mutagenesis Kit (Stratagene) according to the manufacturer's protocols. The pEGFP plasmid harboring the ΔANT(172) sequence was used as a template.

Transient transfection and mammalian two-hybrid assays. COS-7 cells (5×10^5 cells per well in six-well plates) were transiently transfected using a Superfect Transfection Kit (Qiagen). Generally, 2.5 μg of plasmid DNA per well (0.2–1.0 μg of pcDNA3-ANT-1-deletion mutants, 0.2 μg of pCMVhAR [7], and 1.0 μg of pMMTV-luc) was used for the transfection, and the total amount of transfected DNA was kept constant by adding the pcDNA3 plasmid. At 16 h post-transfection, the cells were rinsed in PBS and then cultured in medium containing 10% charcoal-stripped fetal calf serum with or without a steroid hormone (10^{-8} M dihydrotestosterone (DHT)) for an additional 18 h. Subsequently, the cells were harvested and assayed for their luciferase activities using the Dual-Luciferase Reporter Assay System (Promega).

For mammalian two-hybrid assays, NIH3T3 cells were used according to the recommendations included in the Check Mate Mammalian Two-Hybrid System. At 24 h after plating at 10^5 cells per well in 12-well plates, the cells were transiently transfected with 500 ng of pG5luc, 100 ng of VP16 plasmids, and 300 ng of GAL4 plasmids. At 24 h post-transfection, luciferase assays were performed as described above.

Immunoprecipitation. Either COS-AR-AF-1 or COS-7 cells were subjected to transient transfection. Immunoprecipitation was performed as previously described [19]. Briefly, at 24 h post-transfection, whole cell lysates were prepared by lysing the cells in lysis buffer (1.0% Nonidet P-40, 50 mM Tris–HCl, pH 7.8, 150 mM NaCl, 1 mM DTT, and 1 tablet of

protease inhibitor mixture/10 ml buffer). After pre-clearing with protein G–Sepharose beads (Pharmacia), the lysates were incubated with an antibody against c-myc (Santa Cruz Biotechnology) for truncated ANT-1 or an antibody against the NTD of AR N-20 for the truncated ARs in immunoprecipitation (IP) buffer (1.0% Nonidet P-40, 50 mM Tris–HCl, pH 7.8, 200 mM NaCl, 1 mM DTT, and 1 tablet of protease inhibitor mixture/10 ml buffer) at 4 °C for 1 h, and then further incubated with protein G–Sepharose beads at 4 °C for 2 h. The immunoprecipitates were subsequently analyzed by Western blotting using antibodies against AR N-20 or c-myc.

Microscopy and imaging analysis. The cells were divided into 35-mm glass-bottomed dishes (MatTek Corporation) and then transfected with 0.5 μg of the plasmids using 2.5 μl Superfect reagent/dish. At 6–18 h post-transfection, the culture medium was replaced with fresh DMEM. The cells were first imaged without any hormone treatment and then incubated with 10^{-8} M DHT for 1 h. After the incubation, the cells were imaged again using a confocal laser scanning microscope (Leica TCS-SP system; Leica Microsystems). The green fluorescence in the cells was excited using the 488 nm line from an argon laser and the emission was viewed through a 500–550 nm band pass filter.

Results

Activation function and subcellular localizations of ANT-1 deletion mutants

In a previous paper, we demonstrated that an ANT-1 deletion mutant comprised of aa 78–495 (designated ANT-N) showed nearly full enhancement (about 90%) of the ligand-independent AR-AF-1 transactivation capacity of full-length ANT-1, while a deletion mutant comprised of aa 496 to the C-terminus of ANT-1 (designated ANT-C) did not show any enhancement [19]. Therefore, in the present study, ΔANT(499) covering the N-terminal half of ANT-1 was serially deleted from the C-terminal end to generate ΔANT(399), ΔANT(290), ΔANT(172), and ΔANT(146), respectively, in addition to ΔANT(173–499) (Fig. 1A). These fragments were then subcloned into appropriate plasmids to generate plasmids expressing the ANT-1 deletion mutants with and without fusion to GFP. As previously shown, full-length ANT-1 enhanced the transactivation function of the AR, which is activated in the presence of 10^{-8} M DHT, by inducing nearly four-fold enhancement of the AF-1 function. ΔANT(499), ΔANT(399), ΔANT(290), and ΔANT(172) each enhanced the AR-dependent transactivation by about 90% of the level induced by full-length ANT-1, indicating that aa 78–172 are important for the transactivation induced by ANT-1 (Fig. 1B). In contrast, when aa 147–172 were deleted (ΔANT(146)), the transactivation function was almost negligible. This result was further confirmed by the findings that neither ΔANT(173–499) nor ANT-C were able to induce any transactivation.

Next, we investigated the subcellular and intranuclear distributions of the ANT-1 deletion mutants fused in-frame to GFP. Representative confocal microscopic images of COS-7 cells transfected with the expression plasmids for the fusion proteins are shown in Fig. 2. As previously demonstrated, full-length ANT-1-GFP showed two distinct distributions in the nucleus: a diffuse reticular distribution

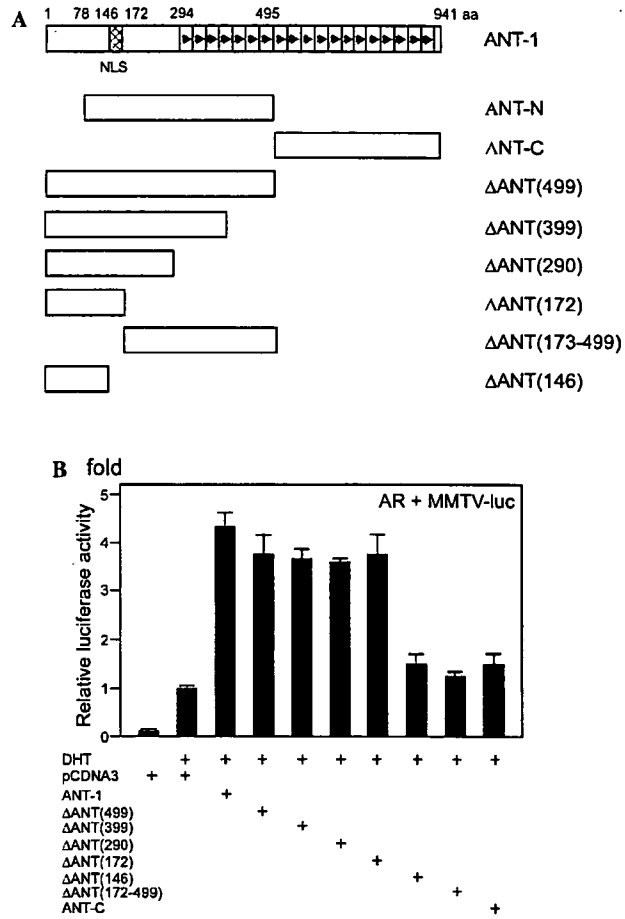

Fig. 1. Schematic diagrams of the human ANT-1 deletion mutants and their transactivation functions. (A) Schematic diagrams of the ANT-1 truncated mutants used in the experiments. The structure of full-length ANT-1 is shown at the top. ANT-1, a binding protein for U5 snRNP, consists of 941 aa and possesses 19 TPR motifs from aa 294 within the last two-thirds of the C-terminal region (shown by arrowheads in open boxes). The putative NLS is shown as a hatched box. ANT-N (aa 78–495) and ANT-C (aa 495–941) were reported previously. All the truncated fragments were subcloned into appropriate plasmids and subjected to reporter assays, confocal microscopic observation, mammalian two-hybrid assays, and immunoprecipitation. (B) Transactivation functions of the truncated mutants of ANT-1. COS-7 cells were transfected with the empty pcDNA3 plasmid (pcDNA3) or pcDNA3 harboring full-length ANT-1 or its deletion mutants (ΔANT(499) to ANT-C), a plasmid expressing the full-length AR (molar ratio 5:1) and a pMMTV-luc reporter plasmid, and then treated with 10^{-8} M DHT. The relative enhancement of the luciferase activity compared with that after co-transfection with the empty pcDNA3 plasmid in the presence of 10^{-8} M DHT is expressed as the -fold induction.

throughout the nucleus and 20–40 coarse subnuclear speckles (Fig. 2A) [19]. ΔANT(499)-GFP and ΔANT(399)-GFP showed similar distributions in the nucleus to the full-length fusion protein (Figs. 2B and C). In contrast, ΔANT(290)-GFP, which lacked aa 290–399, did not form any subnuclear speckles and showed only a diffuse distribution in the nucleus (compare Figs. 2C and D), while retaining the transactivation function on the AR (Fig. 1B). These results suggest that the region required for ANT-1 to

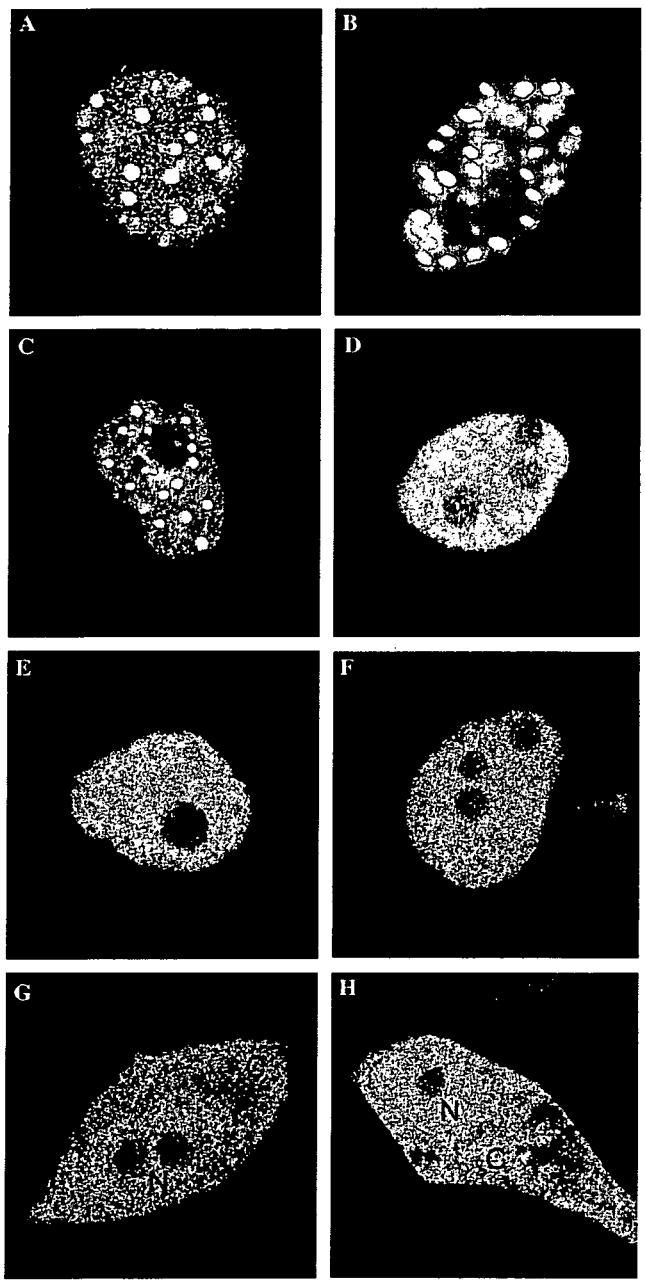

Fig. 2. Confocal microscopic images of the full-length and truncated mutants of ANT-1 fused to GFP. (A–H) COS-7 cells were transiently transfected with pEGFP harboring full-length ANT-1 (A) or its truncated mutants (B–H) and then observed by confocal microscopy. (B) ΔANT(499); (C) ΔANT(399); (D) ΔANT(290); (E) ΔANT(200); (F) ΔANT(172); (G) ΔANT(146); (H) ΔANT(173–499). In addition to the ANT-1 deletion mutants shown in Fig. 1A, a deletion mutant of ANT-1 comprising aa 1–200 (E) was used in the experiments. In (A–F) only the nucleus shows fluorescence. In (G,H) N, nucleus; C, cytoplasm.

generate intranuclear speckles is located between aa 291 and 399, and that speckle formation is not required for the transactivation function of ANT-1. Furthermore, ΔANT(146)-GFP and ΔANT(173–499)-GFP were not concentrated in the nucleus, but diffusely distributed throughout both the nucleus and the cytoplasm, suggesting that the 26 aa sequence from aa 146 to 172 confers nuclear localization (compare Figs. 2F and G).

The NLS and receptor-specific transactivation capacity of ANT-1

The region from aa 145 to 172 contains bipartite basic amino acid stretches, often found in an NLS, separated by a 20 aa interval, namely Lys(146)-Arg(147)-Lys(148) and Lys(169)-Arg(170)-Arg(172). Thus, using the plasmid expressing ΔANT(172)-GFP as a template, we performed site-directed mutagenesis to mutate these basic amino acids in the first stretch alone (ΔANT(172)M1), the second stretch alone (ΔANT(172)M2 and M3), and both stretches (ANT(172)M4 and M5) (Fig. 3A). The mutated plasmids were then transfected into COS-7 cells and observed by confocal microscopy (Fig. 3B). ΔANT(172)M1, ΔANT(172)M2, and ΔANT(172)M3 all showed partial disruption of the nuclear concentration of the fluorescence (panels b–d), thereby generating cytoplasmic fluorescence. When both the first and second stretches were simultaneously mutated, the nuclear translocation of the fusion proteins (ΔANT(172)M4 and ΔANT(172)M5) was almost completely disrupted and resembled that of ΔANT(146) (panels e and f), indicating that these bipartite basic amino acid stretches are the NLS of ANT-1.

When the transactivation capacities of these ΔANT(172) mutants were compared with that of wild-type ΔANT(172), we found that the transactivation function of each mutated fragment was almost completely abolished. As shown in Fig. 3C, even when the nuclear fluorescence was partially disturbed but still much stronger than that in the cytoplasm, the ΔANT(172)M1, ΔANT(172)M2, and ΔANT(172)M3 mutants still did not enhance AR-dependent transactivation. These results indicate that the basic amino acids within this 27 aa sequence may play roles in both the nuclear translocation and the transactivation function of ANT-1.

To test the receptor specificity of the transactivation domain of ANT-1 contained in ΔANT(172), a plasmid expressing ΔANT(172) was transiently transfected into COS-7 cells with an expression plasmid for the AR, GR or ER α. As shown in Fig. 4, co-expression of ΔANT(172) specifically enhanced either the AR or GR, but not ER α, in a dose-dependent manner until the molar ratio of ANT-1:AR was 4:1. When the quantity of the ANT-1 expression plasmid was extremely high (10:1), the TK-driven promoter harboring the estrogen response element or the TK promoter itself was enhanced by twofold. Under these experimental conditions, the AR- or GR-dependent transactivation system was enhanced by 12- to 15-fold. Overall, these results suggest that ΔANT(172) primarily represents the receptor specificity of ANT-1.

ANT-1 binds to AR-AF-1 through TPR motifs

We first performed mammalian two-hybrid assays using AR-AF-1 and ANT-1 deletion mutants. Possibly because

A

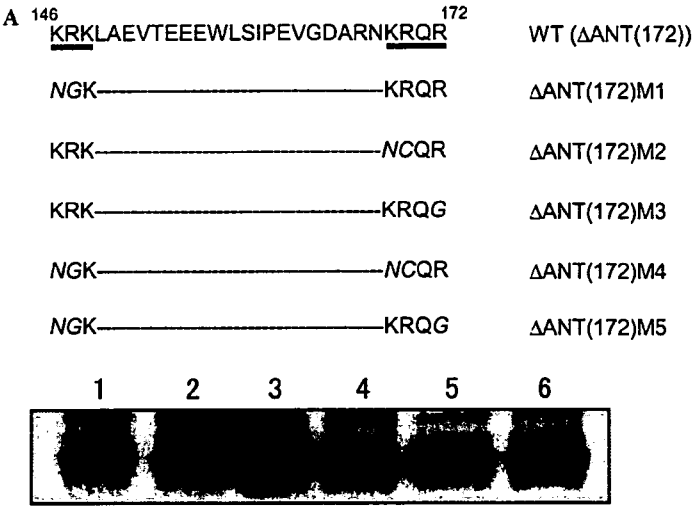
146
KRKLAEVTEEEWLSIPEVGDARNKRQR
172
WT (ΔANT(172))
NGK——————KRQR
ΔANT(172)M1
KRK——————NCQR
ΔANT(172)M2
KRK——————KRQG
ΔANT(172)M3
NGK——————NCQR
ΔANT(172)M4
NGK——————KRQG
ΔANT(172)M5
1 2 3 4 5 6

B

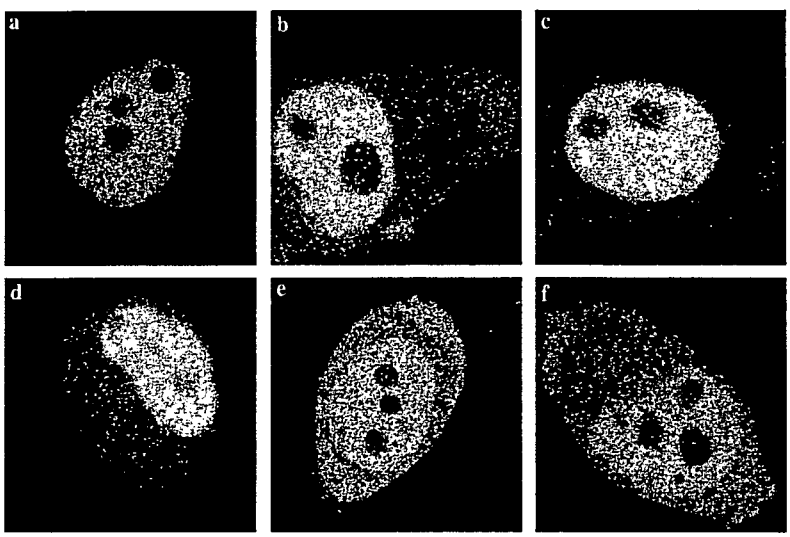
a
b
c
d
e
f

C

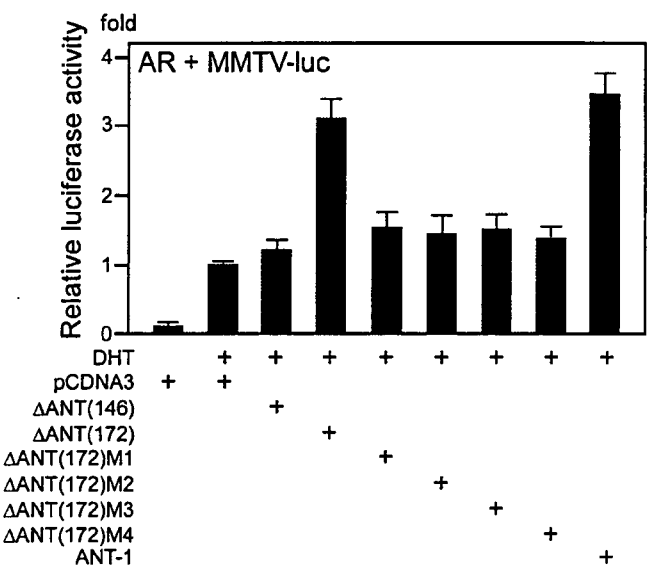
fold
AR + MMTV-luc
Relative luciferase activity
0
1
2
3
4
DHT + + + + + + + + +
pCDNA3 + +
ΔANT(146) +
ΔANT(172) +
ΔANT(172)M1 +
ΔANT(172)M2 +
ΔANT(172)M3 +
ΔANT(172)M4 +
ANT-1 +

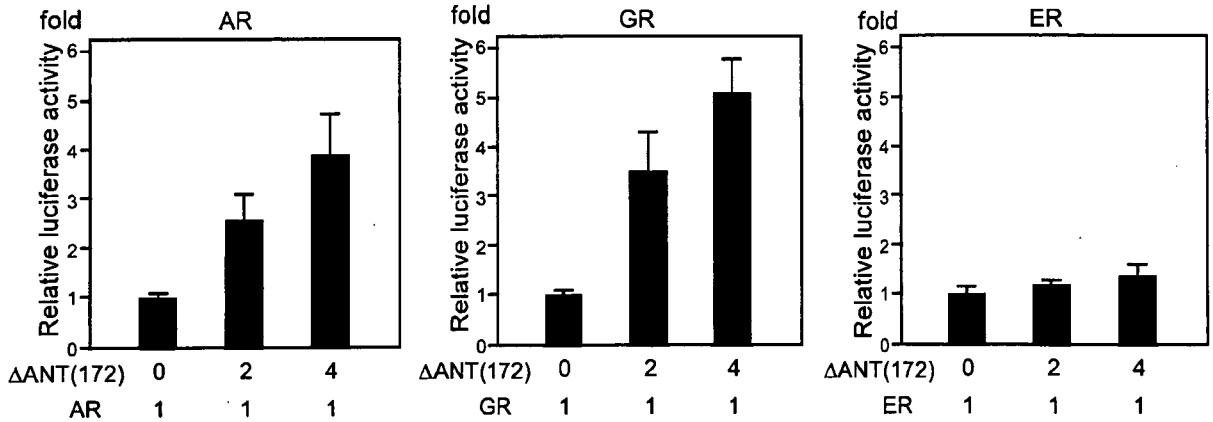

Fig. 4. Receptor-specific transactivation of ΔANT(172). An expression plasmid for ΔANT(172) was transiently transfected into COS-7 cells with expression plasmids for the AR, GR or ER α, together with appropriate reporter plasmids (pMMTV-luc for the AR or GR, and pERE2-tk109-luc for ER α), and then treated with steroid hormones (10^{-8} M DHT, 10^{-7} M dexamethasone or 10^{-8} M estradiol). Co-transfection of the plasmid expressing ΔANT(172) shows specific enhancement of the AR and GR, but not ER α, in a dose-dependent manner until the molar ratio of ANT-1 to the AR or GR reaches 4:1.

AR-AF-1 possesses strong autonomous transactivation capacity, transfection of NIH3T3 cells with the empty VP16 plasmid without any insertion conferred background luciferase activity driven by the GAL-4-containing AR-AF-1 (ΔAR(660)). Therefore, the background activity exerted by the presence of GAL-ΔAR(660) and the VP16 plasmid without an insertion was set as the standard and compared to the activities induced with the VP16 plasmids containing the ANT-1 deletion mutants (Fig. 5). Insertion of full-length ANT-1 into the VP16 plasmid (VP-ANT) or ΔANT(499) truncated in the seventh TPR of the 19 TPR repeats (Fig. 1A) strongly increased the luciferase activities by fivefold. When the sequence from aa 399 (in the fourth TPR) to 499 was deleted, the luciferase activity was weakly increased by twofold. The VP16 plasmid harboring ANT-C, containing 12.5 TPR motifs located at the C-terminal side, also showed about a 2.5-fold increase in the luciferase activity.

Next, we performed immunoprecipitation experiments using lysates of COS-7 cells stably expressing AR-AF-1 (COS-AR-AF-1 cells) transfected with plasmids expressing the ANT-1 deletion mutants tagged with myc. As shown in Fig. 6, only full-length ANT-1 and ΔANT(499) were co-immunoprecipitated with AR-AF-1 (lanes 1 and 2), whereas the other deletion mutants, including ΔANT(399) and ANT-C, were not. Taken together, these results indicate that ANT-1 binds to AR-AF-1 primarily via aa 399–499, encompassing the region from the fourth to the seventh TPR motifs.

ANT-1 binds to the AR sequence between either aa 180–360 or aa 360–532 within AF-1

We created plasmids expressing the AR-AF-1 region divided into three smaller fragments, namely aa 1–180, aa 180–360, and aa 360–532, and performed mammalian two-hybrid assays using ΔAR(660) containing the whole NTD and the DNA-binding domain (DBD) as a control (Fig. 7A). The results revealed that both ΔAR(180–360) and ΔAR(360–532) bound to ΔANT(499), whereas ΔAR(180) did not. Furthermore, the binding was confirmed by immunoprecipitation experiments (Fig. 8). ΔANT(499) was co-immunoprecipitated with either ΔAR(180–360) or ΔAR(360–532) tagged with GAL.

Discussion

We have identified four distinct functional domains in the ANT-1 molecule, which enhances AR-AF-1 transactivation capacity. The four regions were: (1) an NLS

Fig. 3. The nuclear localization signal of ANT-1. (A) Wild-type (WT) and mutant (M1–M5) aa sequences generated by site-directed mutagenesis of ΔANT(172) for expression in COS-7 cells by transient transfection of expression plasmids. Only aa 146–172 are shown. In the WT sequence, the bipartite basic amino acid stretches are underlined. In the sequences of M1–M5, the mutated residue(s) are shown in italics. The lower panel shows the expressions of GFP fusion proteins of WT ΔANT(172) and its mutants in COS-7 cells. Western blot was performed using anti-GFP antibody. Lane 1, WT ΔANT(172); lane 2, ΔANT(172)M1; lane 3, ΔANT(172)M2; lane 4, ΔANT(172)M3; lane 5, ΔANT(172)M4; lane 6, ΔANT(172)M5. (B) Confocal microscopic images of GFP fusion proteins of WT ΔANT(172) and its mutants. COS-7 cells were transiently transfected with plasmids expressing the WT and mutant ΔANT(172)-GFP fusion proteins and then observed by confocal microscopy. (a) WT ΔANT(172); (b) ΔANT(172)M1; (c) ΔANT(172)M2; (d) ΔANT(172)M3; (e) ΔANT(172)M4; (f) ΔANT(172)M5. Mutants M1, M2, and M3 show partial disruption of the nuclear GFP fluorescence, while mutants M4 and M5 show almost complete disruption. (C) Transactivation capacities of WT and mutated ΔANT(172). The cDNA fragments expressing the mutated ΔANT(172)-GFP fusion proteins (M1–M5) were subcloned into pcDNA3 to create expression plasmids for this experiment. COS-7 cells were transfected with the empty pcDNA3 plasmid (pcDNA3) or pcDNA3 expressing the WT or mutated ΔANT(172), or WT ΔANT(146) as a control, together with a plasmid expressing the full-length AR (molar ratio 5:1) and a pMMTV-luc reporter plasmid, and then treated with 10^{-8} M DHT. The relative enhancement of the luciferase activity compared with that after co-transfection with the empty pcDNA3 plasmid in the presence of 10^{-8} M DHT is expressed as the -fold induction.

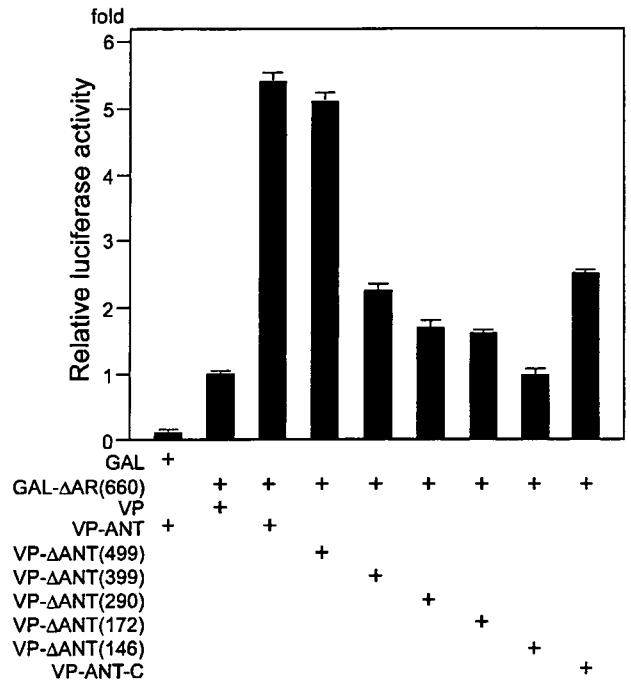

Fig. 5. Mammalian two-hybrid analysis to determine the domain within ANT-1 that binds to AR-AF-1. NIH3T3 cells were transiently transfected with 500 ng of pG5luc, 100 ng of VP16 plasmids containing full-length ANT-1 (VP-ANT) or ANT-1 truncated sequences (see Fig. 1A), and 300 ng of a GAL4 plasmid expressing aa 1–660 of the AR (see Fig. 7A) fused to GAL4. The background activity exerted by the presence of GAL-ΔAR(660) and the VP16 plasmid without an insertion was set as the standard for comparisons with the activities obtained with the VP16 plasmids containing the ANT-1 deletion mutants, and the data are presented as relative activities.

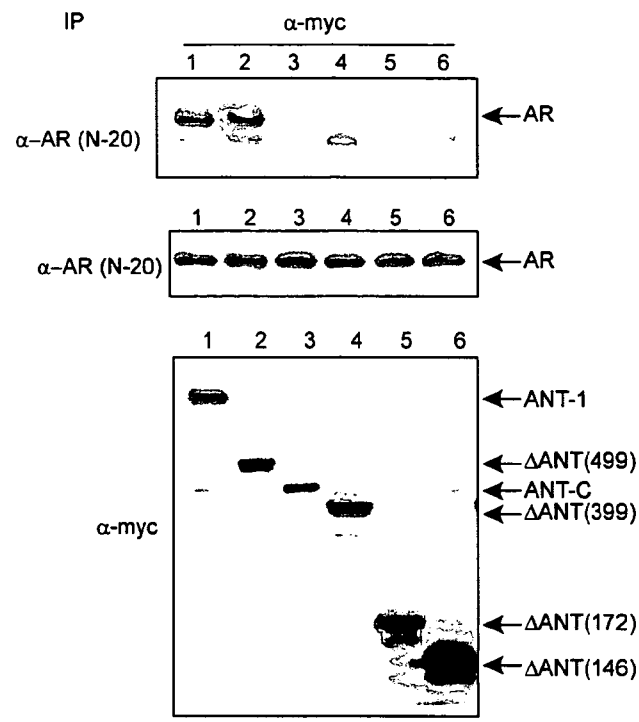

Fig. 6. Immunocoprecipitation of truncated ANT-1 mutants with AR-AF-1. COS-7 cells stably expressing AR-AF-1 (COS-7-AR-AF-1 cells) were transfected with plasmids expressing full-length or truncated mutants of ANT-1 tagged with myc. Immunoprecipitation (IP) was performed using an anti-myc antibody, and the precipitates were analyzed by Western blotting using an antibody against N-20 in AR-AF-1. The middle and bottom panels show the findings for the whole lysates used for the IP as controls. Lanes 1, full-length ANT-1; lanes 2, ΔANT(499); lanes 3, ANT-C; lanes 4, ΔANT(399); lanes 5, ΔANT(172); lanes 6, ΔANT(146).

domain; (2) a receptor-specific AF-1 transactivating domain; (3) an AR-AF-1-binding domain; (4) an intranuclear speckle formation domain. Both the NLS and ANT-1 transactivation domains were within the first 172 aa of the N-terminal region. Furthermore, the NLS of ANT-1 was tightly related to or closely overlapped with the sequence required for the transactivation function of ANT-1. Mutational analysis of the ANT-1 NLS revealed that the transactivation capacities of the intranuclear ANT-1 mutants were almost completely abolished after partial disruption of the nuclear translocation by mutations in either the first or second basic amino acid clusters. Another example of a tight relationship between a bipartite NLS and a transactivation function has been reported for the murine transcription factor distal-less (Dlx) 3, which is involved in the development and differentiation of epithelial tissue [31]. In the Dlx3 protein, the NLS sequences are part of the homeodomain sequence, and thus mutation of the NLS disrupts the sequence required for specific DNA binding, the transactivation potential, and protein–protein interactions [32]. The mechanisms for how the ANT-1 NLS confers the transactivation capacity still remain to be elucidated.

In contrast, the other two domains, required for either binding to AR-AF-1 or intranuclear speckle formation, were present within the first 7 of the 19 TPR motifs found in the ANT-1 molecule. The TPR is a structural motif present in a wide range of proteins and mediates protein–protein interactions for the assembly of multiprotein complexes. The TPR was first identified in 1990, and its name denotes the 34 amino acids comprising the basic repeat [24]. These basic repeats are usually arrayed in a tandem fashion. To date, the TPR motif has been identified in more than 25 proteins, which play important roles in diverse biological functions, including gene transcription and pre-mRNA splicing. The TPR motif has been shown to possess biological significance, since congenital mutations within the motif result in congenital disorders, such as Leber congenital amaurosis [33] and chronic granulomatous disease [34].

ANT-1 is identical to the mammalian nucleoprotein PRP6, which binds to the human splicing factor U5 snRNP (GenBank Accession No. AF221842). During the splicing step, snRNPs play critical roles in constructing the multiprotein–RNA complex known as the spliceosome. The splicing snRNPs (U1, U2, U4/U6, and U5) associate with the pre-mRNA and then with each other in an ordered

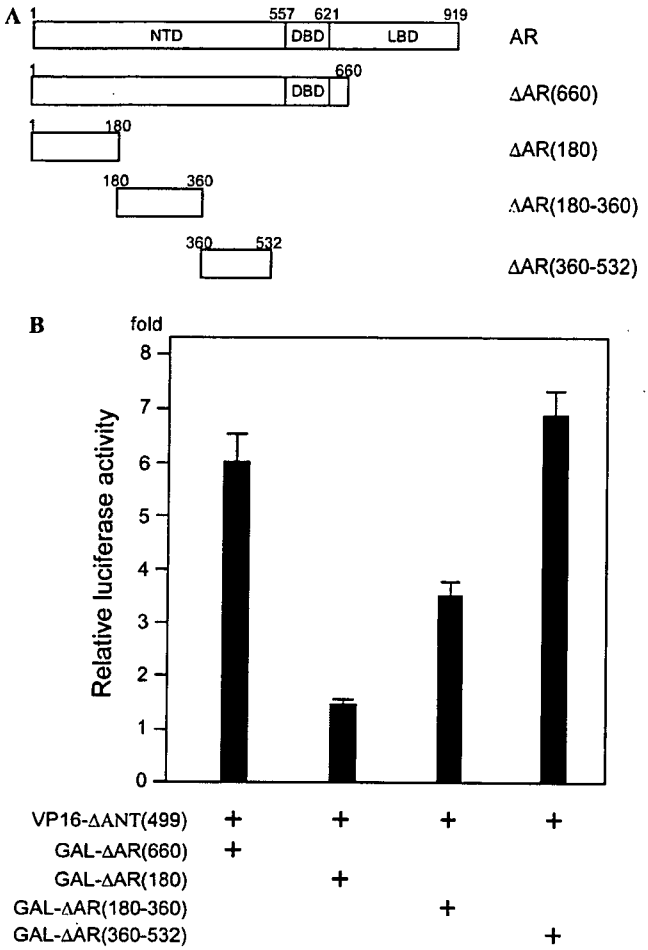

Fig. 7. Mammalian two-hybrid analysis to determine the domain within AR-AF-1 that binds to ANT-1. (A) Schematic diagrams of the truncated mutants of AR-AF-1 used for the experiment. NTD, N-terminal domain; DBD, DNA-binding domain; LBD, ligand-binding domain. (B) Mammalian two-hybrid analysis. NIH3T3 cells were transiently transfected using 500 ng of pG5luc, 100 ng of the VP16 plasmid containing ΔANT(499), or the VP16 plasmid without an insertion as a control, and 300 ng of GAL4 plasmids expressing fusion proteins with truncated mutants of the AR. In each transfection, the background activity exerted by the presence of GAL-ΔARs and the VP16 plasmid without an insertion was set as the standard for comparisons with the activities obtained with the VP16 plasmid containing ΔANT(499), and the data are expressed as the relative activities.

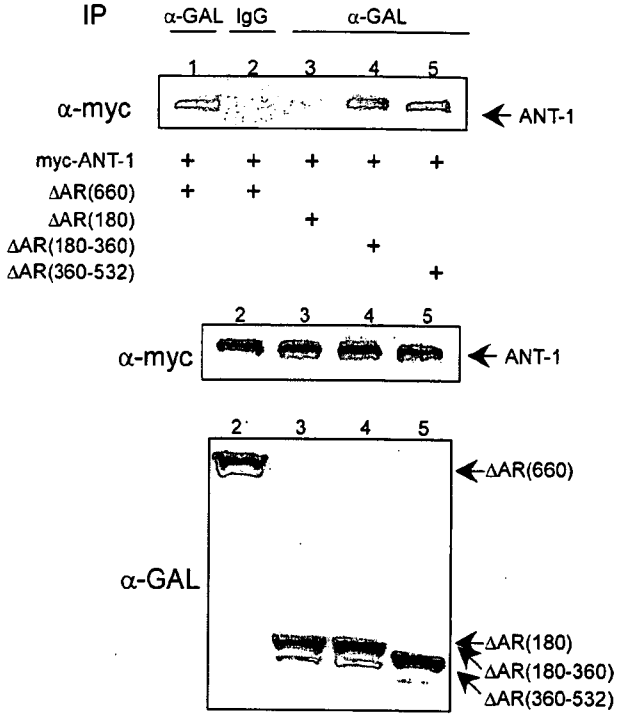

Fig. 8. Immunocoprecipitation of truncated AR mutants with ANT-1. COS-7 cells were transiently transfected with plasmids expressing truncated mutants of the AR tagged with GAL and ΔANT(499) tagged with myc. Immunoprecipitation (IP) was performed using an anti-GAL antibody for lanes 1, 3, 4, and 5 and non-immune IgG (*IgG*) for lane 2 as a control, and the precipitates were analyzed by Western blotting using an anti-myc antibody for ΔANT(499). The middle and bottom panels show the findings for the whole lysates used for the IP as controls. Lanes 1 and 2, ΔAR(660); lanes 3, ΔAR(180); lanes 4, ΔAR(180–360); lanes 5, ΔAR(360–532).

sequence to form the spliceosome, during which U5 snRNA base-pairs with exon sequences flanking the split sites. Through the sequence from aa 290 to 399 at the N-terminal end of the long TPR domain, ANT-1 may bind to the U5 snRNP multiprotein complex in the SFC, thereby forming subnuclear speckles. Although prp6p, a yeast homolog of ANT-1, was originally isolated as a spliceosomal protein, we did not observe any ANT-1-mediated enhancement of the splicing efficiency when assessed using an artificial minigene [19]. Therefore, we previously speculated that ANT-1 per se did not possess any splicing activity, but instead functioned as a transcriptional coactivator. This is in strong contrast to a spliceosomal protein SF3a p120 which is the coactivator specific for ER α-AF1 through the modulation of RNA splicing efficiency via ER α Ser118 phosphorylation [35]. In this regard, ΔANT(172), which may be unable to bind to U5 snRNP due to the absence of all the TPR motifs, showed enhancement of the AR- or GR-dependent transactivation function, but not of ER-dependent transactivation. These findings also indicated that the receptor specificity of the ANT-1-dependent transactivation function was determined by dual mechanisms: (1) via the binding specificity of ANT-1 to cognate receptors such as the AR or GR mediated by the direct binding using TPR motifs; (2) via the receptor-specific enhancement of the transactivation capacity caused by residues between aa 1 and 172, among which aa 146–172 were sufficient for the transactivation function per se. The latter receptor specificity apparently did not require the direct binding to the AR-AF-1, thus it may be exerted by another putative coactivator(s) or enhancer(s) with specific functions.

In good agreement with the subnuclear distribution of prp6p (a yeast homolog of ANT-1) [36], the intranuclear ANT-1 distribution was identical to the known distribution patterns of splicing factors [37]. Transfected ANT-1

showed two distinct distributions in the nucleus as follows: a diffuse fine reticular distribution throughout the nucleus, except for the nucleolus, and a coarsely clustered distribution (speckles) known as the SFC. In a previous paper, we speculated that the subnuclear speckle formation by ANT-1 could be independent of its transactivation function, and thus the merging of the diffuse ANT-1 distribution with the AR speckles may represent the area where ANT-1 or the ANT-1–snRNP complex meets the active AR–cofactor complex [19]. This hypothesis was supported by the current observation that the ANT-1 deletion mutants that were unable to form speckles in the nucleus retained almost the full transactivation capacity for AR-AF-1 (Figs. 1 and 2). Interestingly, mammalian PRP4K kinase (PRP4K) has been shown to be a U5 snRNP-associated kinase that interacts with BRG1, N-CoR, and mammalian PRP6 (ANT-1), and possibly phosphorylates BRG1 and PRP6 [38]. Taken together with our findings, U5 snRNP may play a role in transcription-splicing coupling.

ANT-1 bound to aa 180–360 and 360–532, respectively, within AR-AF-1. Previous studies have assigned AR-AF-1 (also called the transactivation domain or TAD) to aa 142–485 of the receptor. This region comprises both the transcription activation unit (TAU)-1 (aa 101–360) and TAU-5 (aa 360–485) domains [39,40], both of which clearly overlap with the two regions required for binding to ANT-1. Recent studies have revealed that AR-AF-1 lacks a stable secondary structure in aqueous solution, and instead is a structurally flexible polypeptide that folds into a more compact conformation in the presence of structure-stabilizing solutes [41,42]. Hence, the folding of AR-AF-1 in response to specific protein–protein interactions may create a platform for subsequent interactions in the fully competent transactivation complex. This may explain why AR-AF-1 binds many unique proteins, including a subunit of the TFIIF general transcription factor and snRNPs. In this regard, the multiple TPRs present in ANT-1 may play a role in further providing a platform for such interactions.

Acknowledgments

This study was partly supported by Grants-in-Aid for Scientific Research from the Ministry of Education, Culture, Sports, Science and Technology (to K.G. and H.N., respectively) and partly by Core Research for Evolutional Science and Technology from the Japan Science and Technology Agency (to H.N. from 1999 to 2003).

References

[1] M. Beato, S. Chavez, M. Truss, Transcriptional regulation by steroid hormones, Steroids 61 (1996) 240–251.

[2] C.L. Bevan, S. Hoare, F. Claessens, D.M. Heery, M.G. Parker, The AF1 and AF2 domains of the androgen receptor interact with distinct regions of SRC1, Mol. Cell. Biol. 19 (1999) 8383–8392.

[3] P. Alen, F. Claessens, G. Verhoeven, W. Rombauts, B. Peeters, The androgen receptor amino-terminal domain plays a key role in p160 coactivator-stimulated gene transcription, Mol. Cell. Biol. 19 (1999) 6085–6097.

[4] L. Tora, J. White, C. Brou, D. Tasset, N. Webster, E. Scheer, P. Chambon, The human estrogen receptor has two independent nonacidic transcriptional activation functions, Cell 59 (1989) 477–487.

[5] C.A. Quigley, A. De Bellis, K.B. Marschke, M.K. el-Awady, E.M. Wilson, F.S. French, Androgen receptor defects: historical, clinical, and molecular perspectives, Endocr. Rev. 16 (1995) 271–321.

[6] L. Tora, H. Gronemeyer, B. Turcotte, M.P. Gaub, P. Chambon, The N-terminal region of the chicken progesterone receptor specifies target gene activation, Nature 333 (1988) 185–188.

[7] M. Adachi, R. Takayanagi, A. Tomura, K. Imasaki, S. Kato, K. Goto, T. Yanase, S. Ikuyama, H. Nawata, Androgen-insensitivity syndrome as a possible coactivator disease, N. Engl. J. Med. 343 (2000) 856–862.

[8] V.V. Ogryzko, R.L. Schiltz, V. Russanova, B.H. Howard, Y. Nakatani, The transcriptional coactivators p300 and CBP are histone acetyltransferases, Cell 87 (1996) 953–959.

[9] M.L. Lu, M.C. Schneider, Y. Zheng, X. Zhang, J.P. Richie, Caveolin-1 interacts with androgen receptor. A positive modulator of androgen receptor mediated transactivation, J. Biol. Chem. 276 (2001) 13442–13451.

[10] J. Reid, I. Murray, K. Watt, R. Betney, I.J. McEwan, The androgen receptor interacts with multiple regions of the large subunit of general transcription factor TFIIF, J. Biol. Chem. 277 (2002) 41247–41253, Epub 42002 Aug 41213.

[11] X. Yu, P. Li, R.G. Roeder, Z. Wang, Inhibition of androgen receptor-mediated transcription by amino-terminal enhancer of split, Mol. Cell. Biol. 21 (2001) 4614–4625.

[12] S.A. Hayes, M. Zarnegar, M. Sharma, F. Yang, D.M. Peehl, P. ten Dijke, Z. Sun, SMAD3 represses androgen receptor-mediated transcription, Cancer Res. 61 (2001) 2112–2118.

[13] H. Dotzlaw, U. Moehren, S. Mink, A.C. Cato, J.A. Iniguez Lluhi, A. Baniahmad, The amino terminus of the human AR is target for corepressor action and antihormone agonism, Mol. Endocrinol. 16 (2002) 661–673.

[14] P.W. Hsiao, C. Chang, Isolation and characterization of ARA160 as the first androgen receptor N-terminal-associated coactivator in human prostate cells, J. Biol. Chem. 274 (1999) 22373–22379.

[15] S.M. Markus, S.S. Taneja, S.K. Logan, W. Li, S. Ha, A.B. Hittelman, I. Rogatsky, M.J. Garabedian, Identification and characterization of ART-27, a novel coactivator for the androgen receptor N terminus, Mol. Biol. Cell 13 (2002) 670–682.

[16] A. Yamamoto, Y. Hashimoto, K. Kohri, E. Ogata, S. Kato, K. Ikeda, M. Nakanishi, Cyclin E as a coactivator of the androgen receptor, J. Cell Biol. 150 (2000) 873–880.

[17] J.J. Park, R.A. Irvine, G. Buchanan, S.S. Koh, J.M. Park, W.D. Tilley, M.R. Stallcup, M.F. Press, G.A. Coetzee, Breast cancer susceptibility gene 1 (BRCA1) is a coactivator of the androgen receptor, Cancer Res. 60 (2000) 5946–5949.

[18] R.B. Lanz, N.J. McKenna, S.A. Onate, U. Albrecht, J. Wong, S.Y. Tsai, M.J. Tsai, B.W. O'Malley, A steroid receptor coactivator, SRA, functions as an RNA and is present in an SRC-1 complex, Cell 97 (1999) 17–27.

[19] Y. Zhao, K. Goto, M. Saitoh, T. Yanase, M. Nomura, T. Okabe, R. Takayanagi, H. Nawata, Activation function-1 domain of androgen receptor contributes to the interaction between subnuclear splicing factor compartment and nuclear receptor compartment. Identification of the p102 U5 small nuclear ribonucleoprotein particle-binding protein as a coactivator for the receptor, J. Biol. Chem. 277 (2002) 30031–30039, Epub 32002 May 30030.

[20] A. Nishikimi, J. Mukai, N. Kioka, M. Yamada, A novel mammalian nuclear protein similar to *Schizosaccharomyces pombe* Prp1p/Zer1p and *Saccharomyces cerevisiae* Prp6p pre-mRNA splicing factors, Biochim. Biophys. Acta 1435 (1999) 147–152.

[21] E.M. Makarov, O.V. Makarova, T. Achsel, R. Luhrmann, The human homologue of the yeast splicing factor prp6p contains multiple TPR elements and is stably associated with the U5 snRNP via protein–protein interactions, J. Mol. Biol. 298 (2000) 567–575.
[22] W. Seghezzi, K. Chua, F. Shanahan, O. Gozani, R. Reed, E. Lees, Cyclin E associates with components of the pre-mRNA splicing machinery in mammalian cells, Mol. Cell. Biol. 18 (1998) 4526–4536.
[23] K. Ishitani, T. Yoshida, H. Kitagawa, H. Ohta, S. Nozawa, S. Kato, p54nrb acts as a transcriptional coactivator for activation function 1 of the human androgen receptor, Biochem. Biophys. Res. Commun. 306 (2003) 660–665.
[24] L.D. D'Andrea, L. Regan, TPR proteins: the versatile helix, Trends Biochem. Sci. 28 (2003) 655–662.
[25] Y. Xing, C.V. Johnson, P.T. Moen Jr., J.A. McNeil, J. Lawrence, Nonrandom gene organization: structural arrangements of specific pre-mRNA transcription and splicing with SC-35 domains, J. Cell Biol. 131 (1995) 1635–1647.
[26] T. Misteli, D.L. Spector, RNA polymerase II targets pre-mRNA splicing factors to transcription sites in vivo, Mol. Cell 3 (1999) 697–705.
[27] D. Auboeuf, A. Honig, S.M. Berget, B.W. O'Malley, Coordinate regulation of transcription and splicing by steroid receptor coregulators, Science 298 (2002) 416–419.
[28] T. Misteli, Cell biology of transcription and pre-mRNA splicing: nuclear architecture meets nuclear function, J. Cell Sci. 113 (2000) 1841–1849.
[29] A. Tomura, K. Goto, H. Morinaga, M. Nomura, T. Okabe, T. Yanase, R. Takayanagi, H. Nawata, The subnuclear three-dimensional image analysis of androgen receptor fused to green fluorescence protein, J. Biol. Chem. 276 (2001) 28395–28401.
[30] M. Saitoh, R. Takayanagi, K. Goto, A. Fukamizu, A. Tomura, T. Yanase, H. Nawata, The presence of both the amino- and carboxyl-terminal domains in the AR is essential for the completion of a transcriptionally active form with coactivators and intranuclear compartmentalization common to the steroid hormone receptors: a three-dimensional imaging study, Mol. Endocrinol. 16 (2002) 694–706.
[31] A.J. Bendall, C. Abate-Shen, Roles for Msx and Dlx homeoproteins in vertebrate development, Gene 247 (2000) 17–31.
[32] J.T. Bryan, M.I. Morasso, The Dlx3 protein harbors basic residues required for nuclear localization, transcriptional activity and binding to Msx1, J. Cell Sci. 113 (2000) 4013–4023.
[33] M.M. Sohocki, S.J. Bowne, L.S. Sullivan, S. Blackshaw, C.L. Cepko, A.M. Payne, S.S. Bhattacharya, S. Khaliq, S. Qasim Mehdi, D.G. Birch, W.R. Harrison, F.F. Elder, J.R. Heckenlively, S.P. Daiger, Mutations in a new photoreceptor-pineal gene on 17p cause Leber congenital amaurosis, Nat. Genet. 24 (2000) 79–83.
[34] S. Grizot, F. Fieschi, M.C. Dagher, E. Pebay-Peyroula, The active N-terminal region of p67phox. Structure at 1.8 Å resolution and biochemical characterizations of the A128V mutant implicated in chronic granulomatous disease, J. Biol. Chem. 276 (2001) 21627–21631, Epub 22001 Mar 21621.
[35] Y. Masuhiro, Y. Mezaki, M. Sakari, K. Takeyama, T. Yoshida, K. Inoue, J. Yanagisawa, S. Hanazawa, W. O'Malley, B.S. Kato, Splicing potentiation by growth factor signals via estrogen receptor phosphorylation, Proc. Natl. Acad. Sci. USA 102 (2005) 8126–8131, Epub 2005 May 8126.
[36] D.J. Elliott, D.S. Bowman, N. Abovich, F.S. Fay, M. Rosbash, A yeast splicing factor is localized in discrete subnuclear domains, Embo J. 11 (1992) 3731–3736.
[37] T. Misteli, J.F. Caceres, D.L. Spector, The dynamics of a pre-mRNA splicing factor in living cells, Nature 387 (1997) 523–527.
[38] G. Dellaire, E.M. Makarov, J.J. Cowger, D. Longman, H.G. Sutherland, R. Luhrmann, J. Torchia, W.A. Bickmore, Mammalian PRP4 kinase copurifies and interacts with components of both the U5 snRNP and the N-CoR deacetylase complexes, Mol. Cell. Biol. 22 (2002) 5141–5156.
[39] G. Jenster, H.A. van der Korput, J. Trapman, A.O. Brinkmann, Identification of two transcription activation units in the N-terminal domain of the human androgen receptor, J. Biol. Chem. 270 (1995) 7341–7346.
[40] N.L. Chamberlain, D.C. Whitacre, R.L. Miesfeld, Delineation of two distinct type 1 activation functions in the androgen receptor amino-terminal domain, J. Biol. Chem. 271 (1996) 26772–26778.
[41] J. Reid, S.M. Kelly, K. Watt, N.C. Price, I.J. McEwan, Conformational analysis of the androgen receptor amino-terminal domain involved in transactivation. Influence of structure-stabilizing solutes and protein–protein interactions, J. Biol. Chem. 277 (2002) 20079–20086, Epub 22002 Mar 20014.
[42] R. Kumar, E.B. Thompson, Transactivation functions of the N-terminal domains of nuclear hormone receptors: protein folding and coactivator interactions, Mol. Endocrinol. 17 (2003) 1–10.

Available online at www.sciencedirect.com
SCIENCE DIRECT
ELSEVIER
Diabetes Research and Clinical Practice 73 (2006) 322–328
DIABETES RESEARCH AND CLINICAL PRACTICE
www.elsevier.com/locate/diabres

The Gly146Ala variation in human *SF-1* gene: Its association with insulin resistance and type 2 diabetes in Chinese

Wei Liu [a], Min Liu [a], WuQiang Fan [a,b,*], Hajime Nawata [c], Toshihiko Yanase [b]

[a] *Department of Medicine and Endocrinology, Renji Hospital, Shanghai 2nd Medical University, #1630 DongFang Road, PuDong, Shanghai 210127, China*
[b] *Department of Medicine and Bioregulatory Science, Graduate School of Medical Science, Kyushu University, Maidashi 3-1-1, Higashi-ku, Fukuoka 812-8582, Japan*
[c] *Graduate School of Medical Science, Kyushu University, Maidashi 3-1-1, Higashi-ku, Fukuoka 812-8582, Japan*

Received 23 August 2005; accepted 20 February 2006
Available online 27 March 2006

Abstract

Aims: While steroidogenic factor 1 (SF-1) is traditionally an essential nuclear receptor for steroidogenic tissues, current emerging studies revealed that the receptor is also closely implicated in metabolism. Mutations of *SF-1* gene cause metabolic disorders like obesity in both human and mice. The aim of the present study is to examine whether the *Gly*146*Ala* variation in the gene for *SF-1*, that is known to impair SF-1 function and related to adrenal disorders, affects susceptibility to type 2 diabetes.
Methods: Hundred and fifty-one type 2 diabetic subjects and 141 non-diabetic control subjects of Han Chinese were recruited and the *SF-1* genotype were analyzed by PCR-RFLP method.
Results: The *Gly*146*Ala* variation occurs frequently in the Han Chinese. Allele *Ala* frequency in the control subjects (27.3%) was significantly lower than that in type 2 diabetic subjects (37.1%, $\chi^2 = 6.37, p = 0.01$). The *Gly*/*Ala* and *Ala*/*Ala* genotypes frequencies were also higher in diabetic subjects. In both the diabetic and control populations, subjects carrying allele *Ala*, as compared to those not, had higher fasting insulin levels and higher HOMA values.
Conclusions: The *SF-1 Gly*146*Ala* variation may constitute a susceptible factor for development of type 2 diabetes and impairment of insulin actions.

Keywords: Steroidogenic factor 1; Type 2 diabetes; Single nucleotide polymorphism; HOMA

1. Introduction

Steroidogenic factor 1 (SF-1), also known as adrenal 4 binding protein and formally designed as nuclear receptor subfamily 5 group A number 1 (NR5A1), is a monomeric nuclear receptor, that transcriptionally regulates a vast array of genes involved in adrenal and gonadal development, sex differentiation, steroidgenesis and reproduction through out the hypothalamic-pituitary-adrenal/gonad axis [1]. Disruption of *sf-1* gene in mice leads to complete adrenal and gonadal agenesis, impaired function of pituitary gonadatropes and

Abbreviations: AgRP, agouti-related peptide; BMI, body mass index; DBP, diastolic blood pressure; f-IRI: fasting immunoreactive insulin; FPG, fasting plasma glucose; HDL-C, high-density lipoprotein cholesterol; HOMA, homeostasis model assessment; HPA, hypothalamic-pituitary-adrenal; LDL-C, low density lipoprotein cholesterol; NPY, neuropeptide Y; PCR-RFLP, polymerase-chain reaction plus restriction fragment length polymorphism; POMC, pro-opiomelanocortin; SBP, systolic blood pressure; SF-1, steroidogenic factor 1; TC, total cholesterol; TG, triglyceride; VMH, ventromedial hypothalamic; WHR, waist-to-hip ratio

* Corresponding author. Tel.: +86 21 5875 2345x3447; fax: +86 21 5839 4262.
E-mail address: fan_wq@yahoo.com (W. Fan).

0168-8227/$ – see front matter © 2006 Elsevier Ireland Ltd. All rights reserved.
doi:10.1016/j.diabres.2006.02.007

abnormalities of ventromedial hypothalamic nucleus (VMH) [1,2]. Mutations of the gene in human cause congenital adrenal and gonadal disorders as well [3–7].

While SF-1 plays vital roles in steroidogenesis, emerging studies linked the gene to metabolic dishomeostasis. Recent discovery of phospholipids as endogenous ligands for SF-1, make the receptor as a possible nuclear lipid sensor [8,9]. *sf*-1 knockout mice develop late-onset obesity when rescued by adrenal transplantation [10]. All the three adult human *SF-1* gene mutation patients have mild to severe obesity [3,6,7]. Thus impaired *SF-1* function may cause metabolic disorders in both mouse and human.

Functional alterations of human SF-1 caused by mutations may have limited clinical significance since mutations occur very rarely. In contrast, a nonsynonymous single nucleotide polymorphism variation, *Gly*146*Ala* of human *SF-1*, which bears a slightly impaired transactivation, was found occurring frequently in a Japanese population, and had potential clinical importance [11].

To further clarify potential implications of *SF-1* gene function in human metabolic disorders, we analyzed the relationship between human *SF-1 Gly*146*Ala* polymorphism and type 2 diabetes and insulin action in Han Chinese.

2. Materials and methods

2.1. Subjects

A total of 292 Chinese subjects were enrolled in the study. They included 151 subjects with type 2 diabetes and 141 non-diabetic normal control subjects. The diabetic subjects were randomly recruited from patients attending the outpatient clinic of the department of Medicine and Endocrinology, Renji Hospital, Shanghai 2nd Medical University. The diagnosis of type 2 diabetes was based on World Health Organization [12]. Non-diabetic subjects were recruited from an unselected population undergoing routine health checkups at the Renji Hospital. To enhance statistical power to detect association, inclusion criteria as follows were used for non-diabetic subjects: (1) >55 years of age; (2) HBA1C values <6.0%; (3) no family history of type 2 diabetes. All the subjects enrolled in this study were of full Chinese Han ethnicity. The study complied the recommendations of the Declaration of Helsinki, and was performed after obtaining the written informed consent from all the subjects and was approved by the ethics committee of the Shanghai 2nd Medical University.

2.2. Biological measurements

Whole blood samples were drawn in the fasting state, and the fasting plasma glucose (FPG) levels, concentrations of serum lipids, fasting plasma immunoreactive insulin (f-IRI) concentrations (or, C-peptide alternatively, for those who are receiving any sorts of insulin therapy), and HbA1c levels were determined in each subject by standard laboratory techniques calibrated by the uniform standards. Genomic DNA was extracted by kit of QIAamp Blood Maxi Kit (QIAGEN, CA), following the manufacture's protocol. Insulin resistance HOMA: homeostasis model assessment of insulin resistance (HOMA-IR) = fasting insulin (μU/ml) × fasting glucose (mmol/L)/22.5; β-cell function (HOMA-β) = 20 × fasting insulin (μU/ml)/[fasting glucose (mmol/L)-3.5] [13].

2.3. Genotyping of the Gly146Ala polymorphism in SF-1 gene

The *Gly*146*Ala* polymorphism in human *SF-1* gene was genotyped by the polymerase-chain reaction plus restriction fragment length polymorphism (PCR-RFLP) method [11]. In brief, leukocyte genomic DNA was amplified by polymerase-chain reaction with primer flanking exon 4 of human *SF-1* gene, and the PCR products were then digested overnight at 37 °C with the restriction enzyme of *Sph*I. The sequences of the primers are: forward: 5′ CTT AGA GAG GGT GAG TCT GA 3′; reverse: 5′ CTG AAG CCA GTG GGA AGG AT 3′. The annealing temperature was 60 °C. SphI recognizes only the Ala allele and the digestion give rise to one (773 bp) fragment for the Gly allele and two (541 and 232 bp) fragments for the Ala allele. Digest products were resolved by 2% ethidium bromide stained-agarose gel electrophoresis.

2.4. Statistical analysis

Clinical variables are expressed as mean ± standard error of the mean (S.E.M.). Differences in the clinical characteristics between subjects with and without the polymorphism were evaluated by two-tailed Student's *t*-test. The proportions of genotype or alleles were compared by χ^2 analysis. Odds ratio (OR) and 95% confidence interval (CI), non-adjusted and adjusted for age, gender and body mass index (BMI) were calculated by logistic regression analysis. A p value <0.05 was considered as statistically significant. All statistics were analyzed using SPSS for Windows Version 11.0.

3. Results

The characteristics of the type 2 diabetic and non-diabetic control subjects are summarized in Table 1. The clinical features of the type 2 diabetic subjects and non-diabetic control subjects classified according to *SF-1* genotype were shown in Tables 3 and 4, respectively.

The *Gly*146*Ala* human *SF-1* polymorphic variation was relatively frequent in the Han Chinese. 66 of the 141 (46.8%) non-diabetic control subjects contained one or two allele *Ala* (55 *Gly*/*Ala*, 11 *Ala*/*Ala*). The total allele *Ala* frequency was 27.3%, which is much higher

Table 1
Characteristics of the type 2 diabetic (T2DM) and non-diabetic (NDM) subjects enrolled

Characteristics	T2DM	NDM	*p*
n	151	141	–
Gender (male/female)	61/90	34/107	0.003
Age (years)	61.17 ± 0.86	67.31 ± 0.76	0.001
Diabetes onset age	54.95 ± 1.15	–	–
Family history (+/−)	115/36	–	–
BMI (kg/m^2)	26.60 ± 0.37	21.30 ± 0.19	1.13E−28
Waist-to-hip ratio	0.89 ± 0.004	0.82 ± 0.005	6.03E−20
FPG (mmol/l)	9.43 ± 0.49	4.54 ± 0.05	6.12E−22
f-IRI (pmol/l)	21.84 ± 2.34	10.71 ± 0.42	2.80E−05
HOMA-IR	9.29 ± 1.83	2.23 ± 0.09	4.27E−04
HOMA-β	105.19 ± 8.92	258.47 ± 48.09	1.24E−03
SBP (mmHg)	136.03 ± 1.80	128.00 ± 1.33	4.70E−04
DBP (mmHg)	83.39 ± 0.84	81.70 ± 0.80	0.15
TC (mmol/l)	4.93 ± 0.09	5.06 ± 0.07	0.067
TG (mmol/l)	1.73 ± 0.09	1.52 ± 0.09	0.099
HDL-C (mmol/l)	1.35 ± 0.03	1.81 ± 0.04	7.38E−18
LDL-C (mmol/l)	3.18 ± 0.08	3.06 ± 0.08	0.32

than that observed in a healthy Japanese population [11]. Table 2 shows that the allele frequency for the *Ala* variant of the *Gly*146 → *Ala* polymorphism of *SF-1* was significantly higher in the type 2 diabetes group (37.1%) than that in the control group (27.3%, $\chi^2 = 6.37$, $p = 0.01$). A consistent higher genotype frequency of *Gly/Ala* (42.4% in diabetic group versus 39.0% in non-diabetic group) and *Ala/Ala* (15.9% in diabetic group versus 7.8% in non-diabetic group) were also observed ($\chi^2 = 6.22$, $p = 0.04$).

These data indicates that the *Ala*146 *SF-1* variant is associated with increased risk for the development of type 2 diabetes. The OR is 1.57; and 95% CI is 1.11–2.23. The relative risk value is 1.23. This association still exists after adjustment for age, sex, and BMI (OR: 1.56; 95% CI: 1.10–2.31).

The genotypic distribution of the *SF-1 Gly*146*Ala* polymorphism were in Hardy–Weinberg equilibrium both in the non-diabetic and the type 2 diabetic subjects.

In both diabetic and non-diabetic populations, subjects with and without the *Gly*146*Ala* polymorphism were assessed for insulin resistance and β-cell function by the homeostasis model assessment (HOMA-IR and HOMA-β) as described in the Methods. Values obtained from HOMA have been shown to correlate well with those from the glucose clamp technique [14]. For diabetic patients who are receiving any kinds of insulin therapy, fating C-peptide was alternatively measured to assess the endogenous insulin secretion.

Among diabetic patients, although fasting glucose levels were not different between the two sub-groups subjects who carry the *Ala*146 variant or not respectively (Table 3), fasting insulin levels were noticed significantly elevated in the subjects carrying one or two *Ala*146 allele (25.94 ± 3.60) as compared to those *Gly/Gly* subjects (15.01 ± 0.88, $p = 0.02$). The high fasting insulin levels led to significantly higher HOMA-IR and HOMA-β values in subjects carrying the *Ala*146 variant (Table 3).

Type 2 diabetes per se affects on insulin and glucose level, and overt diabetic patients received treatments in forms of diet, oral hypoglycemic agent and/or insulin. Although the treatment profiles are not significantly different between the Ala carrying and non-carrying T2DM subjects (Table 3), those treatments might still to some extent impact on the secretion or sensitivity (or both) of insulin. Therefore we carried out a further analysis to investigate any possible effect of the *Gly*146*Ala* polymorphism on insulin resistance in non-diabetic subjects as well. As shown in Table 4,

Table 2
Genotypic and allelic prevalence of the *SF-1 Gly*146*Ala* polymorphism in type 2 diabetic (T2DM) and non-diabetic (NDM) subjects

	Genotype [*n*, (%)]			χ^2	*p*	Alleles [*n*, (%)]		χ^2	*p*
	Gly/Gly	*Gly/Ala*	*Ala/Ala*			*Gly*	*Ala*		
T2DM [151]	63 (41.7)	64 (42.4)	24 (15.9)	6.22	0.04	190 (62.9)	112 (37.1)	6.37	0.01
NDM [141]	75 (53.2)	55 (39.0)	11 (7.8)			205 (72.7)	77 (27.3)		